State-space Levy solution for size-dependent static, free vibration and buckling behaviours of functionally graded sandwich plates

Luan C. Trinh [a,b], Thuc P. Vo [a,c], Huu-Tai Thai [d,e,f*], Trung-Kien Nguyen [b]

Poologanathan Keerthan[a]

[a] Department of Mechanical and Construction Engineering, Northumbria University, Ellison Place, Newcastle upon Tyne NE1 8ST, UK

[b] Faculty of Civil Engineering, Ho Chi Minh City University of Technology and Education, 1 Vo Van Ngan Street, Thu Duc District, Ho Chi Minh City, Vietnam

[c] Institute of Research and Development, Duy Tan University, 03 Quang Trung, Da Nang, Vietnam

[d] Division of Construction Computation, Institute for Computational Science, Ton Duc Thang University, Ho Chi Minh City, Vietnam

[e] Faculty of Civil Engineering, Ton Duc Thang University, Ho Chi Minh City, Vietnam

[f] School of Engineering and Mathematical Sciences, La Trobe University, Bundoora, VIC 3086, Australia

Abstract

The size-dependent static, free vibration and buckling behaviours of functionally graded (FG) sandwich plates are analysed in this study. Utilising the modified couple stress theory and variational principle, governing equations of motion are developed with a refined shear deformation theory. The rectangular plates embedded on two opposite simply-supported edges with the arbitrary combinations of the other two. Based on the state-space Levy solution, the deflections, stresses, natural frequencies and critical buckling loads are analytically solved for the closed-form formulations. The effects of material distribution and graded schemes, geometric parameters and boundary conditions are also investigated to examine the size-dependent behaviours of FG sandwich microplates.

Keywords: Functionally graded sandwich microplate, state-space based solution, Levy solution, modified couple stress theory, size-dependent behaviours.

* Corresponding author. Tel.: +44 (0) 191 243 7856
E-mail address: thaihuutai@tdt.edu.vn (H.T. Thai); thuc.vo@northumbria.ac.uk (Thuc P. Vo).

Nomenclature

FGM	: functionally graded material
MEMS	: micro-electro-mechanical system
NEMS	: nano-electro-mechanical system
a, *b*, *h*	: geometry of plate
l	: material length scale parameter
p	: power-law index of FGM
Π, K and W	: strain energy, kinetic energy and external work
$\mathscr{V}$	: volume of the body, which can be decomposed to the mid-plane area $A=\left[\frac{-a}{2},\frac{a}{2}\right]\times[0,b]$ and the thickness domain $\left[\frac{-h}{2},\frac{h}{2}\right]$
σ_{ij}, m_{ij}	: stress and couple-stress components
ε_{ij}, χ_{ij}	: strain and micro-curvature components
λ, μ	: Lamé constants of material
$E(z)$, ν	: Young's modulus and Poisson's ratio of material
$u_i=(u_x,u_y,u_z)$	: displacements in the x, y and z directions of an arbitrary point
$\theta_i=(\theta_x,\theta_y,\theta_z)$	: rotations about the x, y and z axes of an arbitrary point
U, V	: in-plance displacements in x and y directions of a point on the mid-plane of plate
W_b, W_s	: bending and shear displacements of a point on the mid-plane of plate
$f(z)=\frac{4}{3}\frac{z^3}{h^2}$	: shape function describing the contribution of the shear displacement across the thickness

1. Introduction

Functionally graded materials (FGMs) are a class of composite materials in which the material properties vary gradually from one position to the other. The gradation process of this kind of materials can create the industrial products with smooth and continuous properties, hence avoids the stress concentration, cracking and delamination phenomena occurred in the conventional composite materials. These striking features are appealing to the researchers in developing the advanced theories and numerical methods to predict accurate behaviours of FGMs. Their applications can be found in aerospace structures [1], cutting tools [2], actuators, transducers [3] and biomedical installations, etc. An insightful introduction to the applications of FGMs is presented in [4]. FG-sandwich structures, which are the combinations of FGMs and sandwich structures, have more attractive characteristic since they can tailor material properties and eliminate the delamination, which occurs in conventional sandwich structures.

Recent developments in technology require the knowledge of small-scale structural elements, which are commonly presented in MEMS and NEMS such as thin films, nano-probes, sensors, actuators and other devices. There have been much developments in manufacturing- and measuring- process for these small-scale FG structures in recent years [5-8], which attract more research in investigating the behaviours of such structures. It is evidenced from experiments [9-11] that when the dimensions of these structures are reduced to a certain value, the size effects in structural behaviours can be observed. There are several approaches to investigate these effects including the experimentation, atomistic/molecular dynamics simulation and higher-order continuum mechanics. Although the two former methods can provide more accurate prediction, the latter has been employed widely due to the computational efficiency. The higher-order continuum theories, which are widely known as the non-classical continua, were initiated in the work of Cosserat and Cosserat [12] in 1909. Utilising the concept of directors, which was a triad of vectors, the additional degrees of freedom (DOF) are introduced apart from the classical DOFs of displacements to state the independent microrotation of material particles. This idea has drawn much attention from scholars since 1960s with the development of various assumptions regarding the constitutive laws and the measuring of such additional DOFs. Although a good number of theories have been proposed with respect to these higher-order continuum theories, three major categories can be summarised covering the microcontinua, nonlocal elasticity and the strain gradient family [13]. The microcontinua were developed by Eringen [14-17] for 3M theories which are the micromorphic, microstretch and micropolar with nine, four and three additional DOFs included, respectively [18]. The nonlocal elasticity was firstly proposed by Kroner [19] and further developed by Eringen [20-22]. In these theories, the stress at a reference point is measured through the constitutive law by the strains around its effective area. Therefore, the size effects are captured by introducing a nonlocal parameter to the constitutive equations. The third class of higher-order continua is the strain gradient family, which are composed of the couple stress theory, the strain gradient theory and their modified versions. In the strain gradient family, the strain energy is considered as a function of both strains and strain gradients, which requires additional material constants, i.e. material length scale parameters, compared to the classical continuum. Mindlin [23] proposed an original strain gradient theory considering the first gradient of strains only and developed another version including both the first and second gradients of strains [24]. In order to improve the efficiency and reduce the material parameters required from experiments, various models based on different strain gradients were examined. In the classical couple stress theories, which were proposed by Toupin [25, 26], Mindlin and Tiersten [27] and Koiter [28], only the gradients of rotation vectors are included, leading to only two additional material length scale parameters required. Later, the modified couple stress theory (MCST) was developed by Yang et al. [29] with the introduction of an equilibrium condition of moments of couples. This higher-order equilibrium enforces the couple stress tensor to be symmetric, hence only one material length scale parameter is required. An interesting discussion on another approach to derive this symmetry of couple stress tensor can be found in the work of Munch et al. [30]. Using the MCST, a large number of publications were developed to investigate structural behaviours of microplates including bending, vibration and buckling based on various shear deformation theories such as the classical plate theory (CPT), first-order shear deformation theory (FSDT) and higher-order shear deformation theory (HSDT). Using the MCST CPT, Asghari and Taati [31] analysed the free vibration of FG microplates with arbitrary shapes. Taati [32] then included the geometric nonlinearity to investigate the buckling and post-buckling behaviours of FG microplates under different boundary conditions (BCs) with an analytical solution. Based on the MCST FSDT, the static, free vibration and buckling behaviours of FG annular microplates with various BCs were investigated by Ke et al. [33]. Thai and Choi [34] developed an analytical solution to linear and nonlinear bending, vibration and buckling behaviours of simply supported FG microplates; later on elastic medium was then included by Jung et al. [35, 36]. Ansari et al. [37, 38] also adopted the differential quadrature (DQ) method for nonlinear vibration, bending and post-buckling analysis of FG microplates. In recent years, the HSDTs and 3D elasticity have been developed extensively to improve the accuracy in predicting structural behaviours of composite and FG structures [39-44]. They also have been applied to investigate the behaviours of microplates. Thai and Kim [45] examined the bending and free vibration behaviours of FG microplates using analytical solutions while such behaviours for the annular/circular microplates was investigated by Eshraghi using DQ method [46]. The MCST sinusoidal shear deformation model was also developed by Thai and Vo [47] for deflections and natural frequencies of simply supported microplates. Some other refined plate models [48, 49] and quasi-3D [50-52] were also employed the MCST for FG microplates. In addition, the thermal effects are examined for the FG microplates in many publications. Using the MSCT CPT, Mirsalehi et al. [53] investigated stability of thin FG microplate under mechanical and thermal load based on spline finite strip method. Ashoori and Vanini [54] also studied thermal buckling of annular FG microplate resting on an elastic medium and extended to geometric nonlinearity effect and snap-through behaviour. Utilising DQ method, Eshaghi et al. [55] analysed static bending and natural frequencies of FG annular/circular employing the MCST CPT, FSDT and HSDT models.

In this paper, a four-variable refined shear deformation theory is developed for static, free vibration and buckling behaviours of FG sandwich microplates. Based on a state space approach, these structural behaviours of micro rectangular plates with two opposite simply-supported sides and arbitrary combinations of boundary conditions on other sides are presented. By this way, the closed-form solutions can be obtained to demonstrate the effect of various boundary conditions to the micro behaviours of FG-sandwich plates for the first time. The effects of geometric parameters, material distribution and graded schemes to the size-dependent behaviours of FG sandwich microplates are also investigated. The governing equations and corresponding boundary conditions together with the tabular results can be used to verify those developed from other numerical methods.

2. Kinematics and constitutive relations

Consider a FG-sandwich plate with the coordinate and cross-section shown in Fig. 1. By applying the MCST, the variation of strain energy in the body $\mathscr{V}$ is related to both strain and curvature tensors as [29]:

$$\delta\Pi = \int_{\mathscr{V}} \left(\sigma_{ij}\delta\varepsilon_{ij} + m_{ij}\delta\chi_{ij} \right) d\mathscr{V} \tag{1}$$

where ε_{ij} and χ_{ij} are the strain and symmetric microcurvature tensor defined by:

$$\varepsilon_{ij} = \frac{1}{2}\left(\frac{\partial u_i}{\partial x_j} + \frac{\partial u_j}{\partial x_i} \right) \tag{2a}$$

$$\chi_{ij} = \frac{1}{2}\left(\frac{\partial \theta_i}{\partial x_j} + \frac{\partial \theta_j}{\partial x_i} \right) \tag{2b}$$

σ_{ij} and m_{ij} are the corresponding stress and deviatoric part of the symmetric couple stress tensors defined by:

$$\sigma_{ij} = \lambda tr\left(\varepsilon_{ij}\right) + 2\mu\varepsilon_{ij} \tag{3a}$$

$$m_{ij} = 2l^2 \mu \chi_{ij} \tag{3b}$$

in which, $\lambda = \dfrac{E\nu}{(1+\nu)(1-2\nu)}$ and $\mu = \dfrac{E}{2(1+\nu)}$ are the Lamé constants, l is the material length scale parameter [29], $u_i = \left(u_x, u_y, u_z\right)$ and $\theta_i = \left(\theta_x, \theta_y, \theta_z\right)$ are the displacement and rotation vectors expressed as follows.

Utilising the refined deformation theory [52, 56], the displacement field of an arbitrary point is described as follows:

$$u_x\left(x,y,z,t\right) = U\left(x,y,t\right) - z\frac{\partial W_b\left(x,y,t\right)}{\partial x} - f\left(z\right)\frac{\partial W_s\left(x,y,t\right)}{\partial x} \tag{4a}$$

$$u_y\left(x,y,z,t\right) = V\left(x,y,t\right) - z\frac{\partial W_b\left(x,y,t\right)}{\partial y} - f\left(z\right)\frac{\partial W_s\left(x,y,t\right)}{\partial y} \tag{4b}$$

$$u_z\left(x,y,z,t\right) = W_b\left(x,y,t\right) + W_s\left(x,y,t\right) \tag{4c}$$

where U and V are in-plane displacements, W_b and W_s are the bending and shear displacements of a point on the mid-plane of plate. $f\left(z\right) = \dfrac{4}{3}\dfrac{z^3}{h^2}$ is the shape function describing the contribution of the shear displacement across the thickness.

The rotation vector is expressed as:

$$\theta_i = \frac{1}{2} curl\, u_i = \frac{1}{2}\left[\left(\frac{\partial \mathrm{u}_z}{\partial y} - \frac{\partial \mathrm{u}_y}{\partial z} \right)\mathbf{e_x} + \left(\frac{\partial \mathrm{u}_x}{\partial z} - \frac{\partial \mathrm{u}_z}{\partial x} \right)\mathbf{e_y} + \left(\frac{\partial \mathrm{u}_y}{\partial x} - \frac{\partial \mathrm{u}_x}{\partial y} \right)\mathbf{e_z} \right] \tag{5a}$$

$$\theta_x = \frac{1}{2} curl\, u_i \Big|_{\mathbf{e}_x} = \frac{\partial W_b}{\partial y} + \frac{1}{2}\left(1 + \frac{\partial f}{\partial z}\right)\frac{\partial W_s}{\partial y} \tag{5b}$$

$$\theta_y = \frac{1}{2} curl\, u_i\big|_{\mathbf{e}_y} = -\frac{\partial W_b}{\partial x} - \frac{1}{2}\left(1+\frac{\partial f}{\partial z}\right)\frac{\partial W_s}{\partial x} \tag{5c}$$

$$\theta_z = \frac{1}{2} curl\, u_i\big|_{\mathbf{e}_z} = \frac{1}{2}\left(\frac{\partial \mathrm{V}}{\partial x} - \frac{\partial \mathrm{U}}{\partial y}\right) \tag{5d}$$

The strain components related to above displacement field are presented by substituting Eq. (4) to Eq. (2a):

$$\varepsilon_{xx} = \frac{\partial U}{\partial x} - z\frac{\partial^2 W_b}{\partial x^2} - f\,\frac{\partial^2 W_s}{\partial x^2} \tag{6a}$$

$$\varepsilon_{yy} = \frac{\partial V}{\partial y} - z\frac{\partial^2 W_b}{\partial y^2} - f\,\frac{\partial^2 W_s}{\partial y^2} \tag{6b}$$

$$\varepsilon_{zz} = 0 \tag{6c}$$

$$\gamma_{xy} = 2\varepsilon_{xy} = \frac{\partial U}{\partial y} + \frac{\partial V}{\partial x} - 2z\frac{\partial^2 W_b}{\partial x \partial y} - 2f\,\frac{\partial^2 W_s}{\partial x \partial y} \tag{6d}$$

$$\gamma_{xz} = 2\varepsilon_{xz} = g\,\frac{\partial W_s}{\partial x} \tag{6e}$$

$$\gamma_{yz} = 2\varepsilon_{yz} = g\,\frac{\partial W_s}{\partial y} \tag{6f}$$

and the curvature tensor is given by substituting Eq. (5) into Eq. (2b):

$$\chi_{xx} = \frac{\partial^2 W_b}{\partial x \partial y} + \frac{1}{2}\left(1+\frac{\partial f}{\partial z}\right)\frac{\partial^2 W_s}{\partial x \partial y} \tag{7a}$$

$$\chi_{yy} = -\frac{\partial^2 W_b}{\partial x \partial y} - \frac{1}{2}\left(1+\frac{\partial f}{\partial z}\right)\frac{\partial^2 W_s}{\partial x \partial y} \tag{7b}$$

$$\chi_{zz} = 0 \tag{7c}$$

$$\chi_{xy} = \frac{1}{2}\left[\frac{\partial^2 W_b}{\partial y^2} - \frac{\partial^2 W_b}{\partial x^2} + \frac{1}{2}\left(1+\frac{\partial f}{\partial z}\right)\left(\frac{\partial^2 W_s}{\partial y^2} - \frac{\partial^2 W_s}{\partial x^2}\right)\right] \tag{7d}$$

$$\chi_{xz} = \frac{1}{4}\left[\frac{\partial^2 \mathrm{V}}{\partial x^2} - \frac{\partial^2 \mathrm{U}}{\partial x \partial y} + \frac{\partial^2 f}{\partial z^2}\frac{\partial W_s}{\partial y}\right] \tag{7e}$$

$$\chi_{yz} = \frac{1}{4}\left[\frac{\partial^2 V}{\partial x \partial y} - \frac{\partial^2 U}{\partial y^2} - \frac{\partial^2 f}{\partial z^2}\frac{\partial W_s}{\partial x}\right] \tag{7f}$$

Substituting Eqs. (6) and (7) to Eq. (3), the stress and deviatoric part of couple stress tensors are obtained, respectively:

$$\begin{Bmatrix} \sigma_{xx} \\ \sigma_{yy} \\ \sigma_{xz} \\ \sigma_{yz} \\ \sigma_{xy} \end{Bmatrix} = \begin{bmatrix} Q_{11} & Q_{12} & 0 & 0 & 0 \\ & Q_{22} & 0 & 0 & 0 \\ & & Q_{44} & 0 & 0 \\ & & & Q_{55} & 0 \\ sym. & & & & Q_{66} \end{bmatrix} \begin{Bmatrix} \frac{\partial U}{\partial x} - z\frac{\partial^2 W_b}{\partial x^2} - f\frac{\partial^2 W_s}{\partial x^2} \\ \frac{\partial V}{\partial y} - z\frac{\partial^2 W_b}{\partial y^2} - f\frac{\partial^2 W_s}{\partial y^2} \\ g\frac{\partial W_s}{\partial x} \\ g\frac{\partial W_s}{\partial y} \\ \frac{\partial U}{\partial y} + \frac{\partial V}{\partial x} - 2z\frac{\partial^2 W_b}{\partial x \partial y} - 2f\frac{\partial^2 W_s}{\partial x \partial y} \end{Bmatrix} \tag{8a}$$

$$\begin{Bmatrix} m_{xx} \\ m_{yy} \\ m_{zz} \\ m_{xz} \\ m_{yz} \\ m_{xy} \end{Bmatrix} = 2l^2\mu \begin{Bmatrix} \frac{\partial^2 W_b}{\partial x \partial y} + \frac{1}{2}\left(1 + \frac{\partial f}{\partial z}\right)\frac{\partial^2 W_s}{\partial x \partial y} \\ -\frac{\partial^2 W_b}{\partial x \partial y} - \frac{1}{2}\left(1 + \frac{\partial f}{\partial z}\right)\frac{\partial^2 W_s}{\partial x \partial y} \\ 0 \\ \frac{1}{4}\left(\frac{\partial^2 V}{\partial x^2} - \frac{\partial^2 U}{\partial x \partial y} + \frac{\partial^2 f}{\partial z^2}\frac{\partial W_s}{\partial y}\right) \\ \frac{1}{4}\left(\frac{\partial^2 V}{\partial x \partial y} - \frac{\partial^2 U}{\partial y^2} - \frac{\partial^2 f}{\partial z^2}\frac{\partial W_s}{\partial x}\right) \\ \frac{1}{2}\left[\frac{\partial^2 W_b}{\partial y^2} - \frac{\partial^2 W_b}{\partial x^2} + \frac{1}{2}\left(1 + \frac{\partial f}{\partial z}\right)\left(\frac{\partial^2 W_s}{\partial y^2} - \frac{\partial^2 W_s}{\partial x^2}\right)\right] \end{Bmatrix} \tag{8b}$$

where $g = 1 - \frac{df}{dz} = 1 - 4\frac{z^2}{h^2}$, and Q_{ij} for the HSDT are presented as follows:

$$Q_{11} = Q_{22} = \frac{E(z)}{1-\nu^2}, Q_{12} = \frac{E(z)\nu}{1-\nu^2}, Q_{44} = Q_{55} = Q_{66} = \frac{E(z)}{2(1+\nu)} \tag{9}$$

3. Variational formulation

The equations of motion are obtained from the variational principle, which states

$$\int_{t_1}^{t_2} \left(\delta K - \delta\Pi - \delta W \right) dt = 0 \tag{10}$$

where $\delta\Pi$, δK and δW denote the variation of strain, kinetic energy and work done by external forces.

The variation of strain energy is rewritten in terms of mid-plane displacements as:

$$\delta\Pi = \int_A \int_{-h/2}^{h/2} \left(\sigma_{ij}\delta\varepsilon_{ij} + m_{ij}\delta\chi_{ij} \right) dzdA$$

$$= \int_A \int_{-h/2}^{h/2} \Big[\left(\sigma_{xx}\delta\varepsilon_{xx} + \sigma_{yy}\delta\varepsilon_{yy} + \sigma_{zz}\delta\varepsilon_{zz} + \sigma_{xz}\delta\gamma_{xz} + \sigma_{yz}\delta\gamma_{yz} + \sigma_{xy}\delta\gamma_{xy} \right)$$
$$+ \left(m_{xx}\delta\chi_{xx} + m_{yy}\delta\chi_{yy} + m_{zz}\delta\chi_{zz} + 2m_{xz}\delta\chi_{xz} + 2m_{yz}\delta\chi_{yz} + 2m_{xy}\delta\chi_{xy} \right) \Big] dzdA$$

$$= \int_A \Bigg[\left(N_{xx}\frac{\partial\delta U}{\partial x} - M_{xx}\frac{\partial^2\delta W_b}{\partial x^2} - P_{xx}\frac{\partial^2\delta W_s}{\partial x^2} \right) + \left(N_{yy}\frac{\partial\delta V}{\partial y} - M_{yy}\frac{\partial^2\delta W_b}{\partial y^2} - P_{yy}\frac{\partial^2\delta W_s}{\partial y^2} \right)$$
$$+ Q_{xz}\frac{\partial\delta W_s}{\partial x} + Q_{yz}\frac{\partial\delta W_s}{\partial y} + N_{xy}\left(\frac{\partial\delta U}{\partial y} + \frac{\partial\delta V}{\partial x} \right) - 2M_{xy}\frac{\partial^2\delta W_b}{\partial x\partial y} - 2P_{xy}\frac{\partial^2\delta W_s}{\partial x\partial y}$$
$$+ R_{xx}\left(\frac{\partial^2\delta W_b}{\partial x\partial y} + \frac{1}{2}\frac{\partial^2\delta W_s}{\partial x\partial y} \right) + \frac{1}{2}\left(S_{xx} - S_{yy} \right)\frac{\partial^2\delta W_s}{\partial x\partial y} - R_{yy}\left(\frac{\partial^2\delta W_b}{\partial x\partial y} + \frac{1}{2}\frac{\partial^2\delta W_s}{\partial x\partial y} \right)$$
$$+ \frac{1}{2}R_{xz}\left(\frac{\partial^2 V}{\partial x^2} - \frac{\partial^2 U}{\partial x\partial y} \right) + \frac{1}{2}R_{yz}\left(\frac{\partial^2 V}{\partial x\partial y} - \frac{\partial^2 U}{\partial y^2} \right) + \frac{1}{2}X_{xz}\frac{\partial W_s}{\partial y} - \frac{1}{2}X_{yz}\frac{\partial W_s}{\partial x}$$
$$+ \frac{1}{2}R_{xy}\left(\frac{\partial^2 W_b}{\partial y^2} - \frac{\partial^2 W_b}{\partial x^2} + \frac{\partial^2 W_s}{\partial y^2} - \frac{\partial^2 W_s}{\partial x^2} \right) + \frac{1}{2}S_{xy}\left(\frac{\partial^2 W_s}{\partial y^2} - \frac{\partial^2 W_s}{\partial x^2} \right) \Bigg] dA \tag{11}$$

where the in-plane stress and couple stress resultants are expressed as:

$$\left(N_{ij}, M_{ij}, P_{ij}, Q_{ij} \right) = \int_{-h/2}^{h/2} \left(1, z, f, g \right) \sigma_{ij} dz \tag{12a}$$

$$\left(R_{ij}, S_{ij}, X_{ij} \right) = \int_{-h/2}^{h/2} \left(1, \frac{\partial f}{\partial z}, \frac{\partial^2 f}{\partial z^2} \right) m_{ij} dz \tag{12b}$$

It is worth noting that the integration through thickness is written in the general form for FG plates. For the sandwich structures, interested readers may refer to the description and relating formulation in recent publications [57-59]. In this paper, the through-thickness integration for z-dependent functionals is carried out by summing up the integrals in each layer, i.e.

$\int_{-\frac{h}{2}}^{\frac{h}{2}} F(z)dz = \int_{h_0}^{h_1} F(z)dz + \int_{h_1}^{h_2} F(z)dz + \int_{h_2}^{h_3} F(z)dz$, where h_0, h_1, h_2 and h_3 are the z-coordinates of bottom, interlaminar and top surfaces, respectively. By substituting Eqs. (8) and (9) into Eq. (12), these resultant components can be described in terms of mid-plane displacements as in Appendix A.

The variation of the work done by the transverse load q and in-plane applied loads P_x^0, P_y^0 and P_{xy}^0 are presented as:

$$\delta W = -\int_A \left\{ \left[P_x^0 \frac{\partial(W_b+W_s)}{\partial x} + P_y^0 \frac{\partial(W_b+W_s)}{\partial y} \right] \delta(W_b+W_s) \right.$$

$$\left. + P_{xy}^0 \left[\frac{\partial(W_b+W_s)}{\partial x}\frac{\partial\delta(W_b+W_s)}{\partial y} + \frac{\partial(W_b+W_s)}{\partial y}\frac{\partial\delta(W_b+W_s)}{\partial x} \right] + q\delta(W_b+W_s) \right\} dA \tag{13}$$

The variation of kinetic energy is presented by:

$$\delta K = \int_A \int_{-h/2}^{h/2} \rho(z)(\dot{u}_1\delta\dot{u}_1 + \dot{u}_2\delta\dot{u}_2 + \dot{u}_3\delta\dot{u}_3)\,dzdA$$

$$= \int_A \left\{ I_0\left[\dot{U}\delta\dot{U} + \dot{V}\delta\dot{V} + (\dot{W}_b+\dot{W}_s)\delta(\dot{W}_b+\dot{W}_s) \right] - I_1\left(\dot{U}\frac{\partial\delta\dot{W}_b}{\partial x} + \frac{\partial\dot{W}_s}{\partial x}\delta\dot{U} + \dot{V}\frac{\partial\delta\dot{W}_b}{\partial y} + \frac{\partial\dot{W}_b}{\partial y}\delta\dot{V} \right) \right.$$

$$+ I_2\left(\frac{\partial\dot{W}_b}{\partial x}\frac{\partial\delta\dot{W}_b}{\partial x} + \frac{\partial\dot{W}_b}{\partial y}\frac{\partial\delta\dot{W}_b}{\partial y} \right) - J_1\left(\dot{U}\frac{\partial\delta\dot{W}_s}{\partial x} + \frac{\partial\dot{W}_s}{\partial x}\delta\dot{U} + \dot{V}\frac{\partial\delta\dot{W}_s}{\partial y} + \frac{\partial\dot{W}_s}{\partial y}\delta\dot{V} \right) \tag{14}$$

$$\left. + K_2\left(\frac{\partial\dot{W}_s}{\partial x}\frac{\partial\delta\dot{W}_s}{\partial x} + \frac{\partial\dot{W}_s}{\partial y}\frac{\partial\delta\dot{W}_s}{\partial y} \right) + J_2\left(\frac{\partial\dot{W}_b}{\partial x}\frac{\partial\delta\dot{W}_s}{\partial x} + \frac{\partial\dot{W}_s}{\partial x}\frac{\partial\delta\dot{W}_b}{\partial x} + \frac{\partial\dot{W}_b}{\partial y}\frac{\partial\delta\dot{W}_s}{\partial y} + \frac{\partial\dot{W}_s}{\partial y}\frac{\partial\delta\dot{W}_b}{\partial y} \right) \right\} dA$$

where $(I_0, I_1, I_2, J_1, J_2, K_2) = \int_{-h/2}^{h/2} (1, z, z^2, f, zf, f^2)\rho(z)dz$ (15)

Substituting Eqs. (11), (13) and (14) into Eq. (10), performing the integration by parts, the equations of motion can be obtained:

$$\frac{\partial N_{xx}}{\partial x} + \frac{\partial N_{xy}}{\partial y} + \frac{1}{2}\frac{\partial^2 R_{xz}}{\partial x \partial y} + \frac{1}{2}\frac{\partial^2 R_{yz}}{\partial y^2} = I_0\ddot{U} - I_1\frac{\partial \ddot{W}_b}{\partial x} - J_1\frac{\partial \ddot{W}_s}{\partial x} \tag{16a}$$

$$\frac{\partial N_{yy}}{\partial y}+\frac{\partial N_{xy}}{\partial x}-\frac{1}{2}\frac{\partial^2 R_{xz}}{\partial x^2}-\frac{1}{2}\frac{\partial^2 R_{yz}}{\partial x\partial y}=I_0\ddot{V}-I_1\frac{\partial \ddot{W}_b}{\partial y}-J_1\frac{\partial \ddot{W}_s}{\partial y} \tag{16b}$$

$$\frac{\partial^2 M_{xx}}{\partial x^2}+\frac{\partial^2 M_{yy}}{\partial y^2}+2\frac{\partial^2 M_{xy}}{\partial x\partial y}-\frac{\partial^2 R_{xx}}{\partial x\partial y}+\frac{\partial^2 R_{yy}}{\partial x\partial y}-\frac{\partial^2 R_{xy}}{\partial y^2}+\frac{\partial^2 R_{xy}}{\partial x^2}+P(w)+q$$

$$=I_0\left(\ddot{W}_b+\ddot{W}_s\right)+I_1\left(\frac{\partial \ddot{U}}{\partial x}+\frac{\partial \ddot{V}}{\partial y}\right)-I_2\nabla^2\ddot{W}_b-J_2\nabla^2\ddot{W}_s \tag{16c}$$

$$\frac{\partial^2 P_{xx}}{\partial x^2}+\frac{\partial^2 P_{yy}}{\partial y^2}+\frac{\partial Q_{yz}}{\partial y}+\frac{\partial Q_{xz}}{\partial x}+2\frac{\partial^2 P_{xy}}{\partial x\partial y}-\frac{1}{2}\frac{\partial^2 R_{xx}}{\partial x\partial y}-\frac{1}{2}\frac{\partial^2 S_{xx}}{\partial x\partial y}+\frac{1}{2}\frac{\partial^2 R_{yy}}{\partial x\partial y}+\frac{1}{2}\frac{\partial^2 S_{yy}}{\partial x\partial y}$$
$$+\frac{1}{2}\frac{\partial X_{xz}}{\partial y}-\frac{1}{2}\frac{\partial X_{yz}}{\partial x}-\frac{1}{2}\frac{\partial^2 R_{xy}}{\partial y^2}-\frac{1}{2}\frac{\partial^2 S_{xy}}{\partial y^2}+\frac{1}{2}\frac{\partial^2 R_{xy}}{\partial x^2}+\frac{1}{2}\frac{\partial^2 S_{xy}}{\partial x^2}+P(w)+q$$

$$=I_0\left(\ddot{W}_b+\ddot{W}_s\right)+J_1\left(\frac{\partial \ddot{U}}{\partial x}+\frac{\partial \ddot{V}}{\partial y}\right)-J_2\nabla^2\ddot{W}_b-K_2\nabla^2\ddot{W}_s \tag{16d}$$

where $\nabla^2=\frac{\partial^2}{\partial x^2}+\frac{\partial^2}{\partial y^2}$, $P(w)=P_x^0\frac{\partial^2\left(W_b+W_s\right)}{\partial x^2}+P_y^0\frac{\partial^2\left(W_b+W_s\right)}{\partial y^2}+2P_{xy}^0\frac{\partial^2\left(W_b+W_s\right)}{\partial x\partial y}$ (5)

The governing equation can be obtained by substituting the appropriate stress resultants to Eq. (16):

$$A_{11}\frac{\partial^2 U}{\partial x^2}+A_{66}\frac{\partial^2 U}{\partial y^2}-\frac{1}{4}A_m\left(\frac{\partial^4 U}{\partial x^2\partial y^2}+\frac{\partial^4 U}{\partial y^4}\right)+\left(A_{12}+A_{66}\right)\frac{\partial^2 V}{\partial x\partial y}+\frac{1}{4}A_m\left(\frac{\partial^4 V}{\partial x^3\partial y}+\frac{\partial^4 V}{\partial x\partial y^3}\right)$$

$$-B_{11}\frac{\partial^3 W_b}{\partial x^3}-\left(B_{12}+2B_{66}\right)\frac{\partial^3 W_b}{\partial x\partial y^2}-B_{11}^s\frac{\partial^3 W_s}{\partial x^3}-\left(B_{12}^s+2B_{66}^s\right)\frac{\partial^3 W_s}{\partial x\partial y^2}=I_0\ddot{U}-I_1\frac{\partial \ddot{W}_b}{\partial x}-J_1\frac{\partial \ddot{W}_s}{\partial x} \tag{18a}$$

$$A_{22}\frac{\partial^2 V}{\partial y^2}+A_{66}\frac{\partial^2 V}{\partial x^2}-\frac{1}{4}A_m\left(\frac{\partial^4 V}{\partial x^4}+\frac{\partial^4 V}{\partial x^2\partial y^2}\right)+\left(A_{12}+A_{66}\right)\frac{\partial^2 U}{\partial x\partial y}+\frac{1}{4}A_m\left(\frac{\partial^4 U}{\partial x^3\partial y}+\frac{\partial^4 U}{\partial x\partial y^3}\right)$$

$$-B_{22}\frac{\partial^3 W_b}{\partial y^3}-\left(B_{12}+2B_{66}\right)\frac{\partial^3 W_b}{\partial x^2\partial y}-B_{22}^s\frac{\partial^3 W_s}{\partial y^3}-\left(B_{12}^s+2B_{66}^s\right)\frac{\partial^3 W_s}{\partial x^2\partial y}=I_0\ddot{V}-I_1\frac{\partial \ddot{W}_b}{\partial y}-J_1\frac{\partial \ddot{W}_s}{\partial y} \tag{18b}$$

$$B_{11}\frac{\partial^3 U}{\partial x^3}+\left(B_{12}+2B_{66}\right)\frac{\partial^3 U}{\partial x\partial y^2}+\left(B_{12}+2B_{66}\right)\frac{\partial^3 V}{\partial x^2\partial y}+B_{22}\frac{\partial^3 V}{\partial y^3}-\left(D_{11}+A_m\right)\frac{\partial^4 W_b}{\partial x^4}$$
$$-\left(2D_{12}+4D_{66}+2A_m\right)\frac{\partial^4 W_b}{\partial x^2\partial y^2}-\left(D_{22}+A_m\right)\frac{\partial^4 W_b}{\partial y^4}-\left[D_{11}^s+\frac{1}{2}\left(A_m+B_m\right)\right]\frac{\partial^4 W_s}{\partial x^4}$$
$$-\left(2D_{12}^s+4D_{66}^s\right)\frac{\partial^4 W_s}{\partial x^2\partial y^2}-\left[D_{22}^s+\frac{1}{2}\left(A_m+B_m\right)\right]\frac{\partial^4 W_s}{\partial y^4}+P(w)+q$$

$$= I_0\left(\ddot{W}_b + \ddot{W}_s\right) + I_1\left(\frac{\partial \ddot{U}}{\partial x} + \frac{\partial \ddot{V}}{\partial y}\right) - I_2\nabla^2\ddot{W}_b - J_2\nabla^2\ddot{W}_s \tag{18c}$$

$$B_{11}^s \frac{\partial^3 U}{\partial x^3} + \left(B_{12}^s + 2B_{66}^s\right)\frac{\partial^3 U}{\partial x \partial y^2} + \left(B_{12}^s + 2B_{66}^s\right)\frac{\partial^3 V}{\partial x^2 \partial y} + B_{22}^s \frac{\partial^3 V}{\partial y^3}$$
$$-\left[D_{11}^s + \frac{1}{2}\left(A_m + B_m\right)\right]\frac{\partial^4 W_b}{\partial x^4} - \left(2D_{12}^s + 4D_{66}^s\right)\frac{\partial^4 W_b}{\partial x^2 \partial y^2} - \left[D_{22}^s + \frac{1}{2}\left(A_m + B_m\right)\right]\frac{\partial^4 W_b}{\partial y^4}$$
$$+\left(A_{55}^s + \frac{1}{4}H_m\right)\frac{\partial^2 W_s}{\partial x^2} + \left(A_{44}^s + \frac{1}{4}H_m\right)\frac{\partial^2 W_s}{\partial y^2} - \left[H_{11} + \frac{1}{4}\left(A_m + 2B_m + C_m\right)\right]\frac{\partial^4 W_s}{\partial x^4}$$
$$-\left(2H_{12} + 4H_{66}\right)\frac{\partial^4 W_s}{\partial x^2 \partial y^2} - \left[H_{22} + \frac{1}{4}\left(A_m + 2B_m + C_m\right)\right]\frac{\partial^4 W_s}{\partial y^4} + P\left(w\right) + q$$

$$= I_0\left(\ddot{W}_b + \ddot{W}_s\right) + J_1\left(\frac{\partial \ddot{U}}{\partial x} + \frac{\partial \ddot{V}}{\partial y}\right) - J_2\nabla^2\ddot{W}_b - K_2\nabla^2\ddot{W}_s\,. \tag{18d}$$

The expressions for boundary conditions are described by:

$$\delta U : N_{xx}n_x + N_{xy}n_y + \frac{1}{2}\left(\frac{\partial R_{xz}}{\partial y} + \frac{\partial R_{yz}}{\partial x}\right)n_y \tag{19a}$$

$$\delta V : N_{yy}n_y + N_{xy}n_x - \frac{1}{2}\left(\frac{\partial R_{xz}}{\partial x} + \frac{\partial R_{yz}}{\partial y}\right)n_x \tag{19b}$$

$$\delta \frac{\partial V}{\partial x} : R_{xz}n_x + R_{yz}n_y \tag{19c}$$

$$\delta W_b : \frac{\partial M_{xx}}{\partial x} + \frac{\partial M_{xy}}{\partial y} + \frac{\partial R_{xy}}{\partial x} - I_1\ddot{U} + I_2\frac{\partial \ddot{W}_b}{\partial x} + J_2\frac{\partial \ddot{W}_s}{\partial x} + \tilde{P} + \frac{\partial \bar{M}_{ns}}{\partial s} \tag{19d}$$

$$\delta \frac{\partial W_b}{\partial n} : \bar{M}_{nn} \tag{19e}$$

$$\delta W_s : \frac{\partial P_{xx}}{\partial x} + \frac{\partial P_{xy}}{\partial y} + Q_{xz} - \frac{1}{2}X_{yz} + \frac{\frac{1}{2}\partial\left(R_{xy} + S_{xy}\right)}{\partial x} + \frac{\frac{1}{2}\partial\left(R_{yy} + S_{yy}\right)}{\partial y} + \tilde{P} + \frac{\partial \bar{P}_{ns}}{\partial s}$$
$$-J_1\ddot{U} + J_2\frac{\partial \ddot{W}_b}{\partial x} + K_2\frac{\partial \ddot{W}_s}{\partial x} = 0 \tag{19f}$$

$$\delta \frac{\partial W_s}{\partial n} : \bar{P}_{nn} \tag{19g}$$

where

$$\tilde{P}=\left[P_x^0\frac{\partial\left(W_b+W_s\right)}{\partial x}+P_{xy}^0\frac{\partial\left(W_b+W_s\right)}{\partial y}\right]n_x+\left[P_{xy}^0\frac{\partial\left(W_b+W_s\right)}{\partial x}+P_y^0\frac{\partial\left(W_b+W_s\right)}{\partial y}\right]n_y \tag{20a}$$

$$\bar{M}_{nn}=\left(M_x+R_{xy}\right)n_x^2+\left(M_y-R_{xy}\right)n_y^2+\left(2M_{xy}-R_x+R_y\right)n_xn_y \tag{20b}$$

$$\bar{M}_{ns}=\left(M_y-M_x-2P_{xy}\right)n_xn_y+\left(M_{xy}-R_x\right)n_x^2-\left(M_{xy}+R_y\right)n_y^2 \tag{20c}$$

$$\bar{P}_{nn}=\left(P_x+\frac{1}{2}R_{xy}+\frac{1}{2}S_{xy}\right)n_x^2+\left(P_y-\frac{1}{2}R_{xy}-\frac{1}{2}S_{xy}\right)n_y^2$$

$$+\left(2P_{xy}-\frac{1}{2}R_x-\frac{1}{2}S_x+\frac{1}{2}R_y+\frac{1}{2}S_y\right)n_xn_y \tag{20d}$$

$$\bar{P}_{ns}=\left(P_y-P_x-R_{xy}-S_{xy}\right)n_xn_y+\left(P_{xy}-\frac{1}{2}R_x-\frac{1}{2}S_x\right)n_x^2-\left(P_{xy}+\frac{1}{2}R_y+\frac{1}{2}S_y\right)n_y^2 \tag{20e}$$

Based on the state space solution [60] for the plate with simply supported BCs at $y=0$ and $y=b$, the displacements are expressed in terms of Fourier series as:

$$U\left(x,y\right)=\sum_{n=1}^{\infty}U_n\left(x\right)e^{i\omega t}\sin\beta y \tag{21a}$$

$$V\left(x,y\right)=\sum_{n=1}^{\infty}V_n\left(x\right)e^{i\omega t}\sin\beta y \tag{21b}$$

$$W_b\left(x,y\right)=\sum_{n=1}^{\infty}W_{bn}\left(x\right)e^{i\omega t}\sin\beta y \tag{21c}$$

$$W_s\left(x,y\right)=\sum_{n=1}^{\infty}W_{sn}\left(x\right)e^{i\omega t}\sin\beta y \tag{21d}$$

where $\beta=n\pi/b$. (22)

By substituting Eq. (21) to Eq. (18), the highest-order of derivatives are expressed by the lower-order and displacements themselves as follow:

$$\frac{\partial^2U_n}{\partial x^2}=a_1U_n+a_2\frac{\partial V_n}{\partial x}+a_3\frac{\partial^3V_n}{\partial x^3}+a_4\frac{\partial W_{bn}}{\partial x}+a_5\frac{\partial^3W_{bn}}{\partial x^3}+a_6\frac{\partial W_{sn}}{\partial x}+a_7\frac{\partial^3W_{sn}}{\partial x^3} \tag{23a}$$

$$\frac{\partial^4V_n}{\partial x^4}=r_1\frac{\partial U_n}{\partial x}+r_2V_x+r_3\frac{\partial^2V_n}{\partial x^2}+r_4W_{bx}+r_5\frac{\partial^2W_{bn}}{\partial x^2}+r_6W_{sx}+r_7\frac{\partial^2W_{sn}}{\partial x^2}+r_8 \tag{23b}$$

$$\frac{\partial^4 W_{bn}}{\partial x^4} = s_1 \frac{\partial U_n}{\partial x} + s_2 V_x + s_3 \frac{\partial^2 V_n}{\partial x^2} + s_4 W_{bx} + s_5 \frac{\partial^2 W_{bn}}{\partial x^2} + s_6 W_{sx} + s_7 \frac{\partial^2 W_{sn}}{\partial x^2} + s_8 \quad (23c)$$

$$\frac{\partial^4 W_{sn}}{\partial x^4} = t_1 \frac{\partial U_n}{\partial x} + t_2 V_x + t_3 \frac{\partial^2 V_n}{\partial x^2} + t_4 W_{bx} + t_5 \frac{\partial^2 W_{bn}}{\partial x^2} + t_6 W_{sx} + t_7 \frac{\partial^2 W_{sn}}{\partial x^2} + t_8 \quad (23d)$$

The coefficients of Eq. (23) are presented in Appendix B.

Eq. (23) can be rewritten in the matrix form as:

$$\frac{\partial \mathbf{Z}(x)}{\partial x} = \mathbf{T}\mathbf{Z}(x) + \mathbf{F}(x) \quad (24)$$

where the vector of variables is

$$\mathbf{Z}(x) = \left\{ U, \frac{\partial U}{\partial x}, V, \frac{\partial V}{\partial x}, \frac{\partial^2 V}{\partial x^2}, \frac{\partial^3 V}{\partial x^3}, W_b, \frac{\partial W_b}{\partial x}, \frac{\partial^2 W_b}{\partial x^2}, \frac{\partial^3 W_b}{\partial x^3}, W_s, \frac{\partial W_s}{\partial x}, \frac{\partial^2 W_s}{\partial x^2}, \frac{\partial^3 W_s}{\partial x^3} \right\}^T ; \quad (25)$$

and matrix **T** are defined as:

$$\mathbf{T} = \begin{bmatrix} 0 & 1 & 0 & 0 & 0 & 0 & 0 & 0 & 0 & 0 & 0 & 0 & 0 & 0 \\ a_1 & 0 & 0 & a_2 & 0 & a_3 & 0 & a_4 & 0 & a_5 & 0 & a_6 & 0 & a_7 \\ 0 & 0 & 0 & 1 & 0 & 0 & 0 & 0 & 0 & 0 & 0 & 0 & 0 & 0 \\ 0 & 0 & 0 & 0 & 1 & 0 & 0 & 0 & 0 & 0 & 0 & 0 & 0 & 0 \\ 0 & 0 & 0 & 0 & 0 & 1 & 0 & 0 & 0 & 0 & 0 & 0 & 0 & 0 \\ 0 & r_1 & r_2 & 0 & r_3 & 0 & r_4 & 0 & r_5 & 0 & r_6 & 0 & r_7 & 0 \\ 0 & 0 & 0 & 0 & 0 & 0 & 0 & 1 & 0 & 0 & 0 & 0 & 0 & 0 \\ 0 & 0 & 0 & 0 & 0 & 0 & 0 & 0 & 1 & 0 & 0 & 0 & 0 & 0 \\ 0 & 0 & 0 & 0 & 0 & 0 & 0 & 0 & 0 & 1 & 0 & 0 & 0 & 0 \\ 0 & s_1 & s_2 & 0 & s_3 & 0 & s_4 & 0 & s_5 & 0 & s_6 & 0 & s_7 & 0 \\ 0 & 0 & 0 & 0 & 0 & 0 & 0 & 0 & 0 & 0 & 0 & 1 & 0 & 0 \\ 0 & 0 & 0 & 0 & 0 & 0 & 0 & 0 & 0 & 0 & 0 & 0 & 1 & 0 \\ 0 & 0 & 0 & 0 & 0 & 0 & 0 & 0 & 0 & 0 & 0 & 0 & 0 & 1 \\ 0 & t_1 & t_2 & 0 & t_3 & 0 & t_4 & 0 & t_5 & 0 & t_6 & 0 & t_7 & 0 \end{bmatrix} \quad (26)$$

and the force vector in static bending is described by:

$$\mathbf{F}(x) = \{0 \;\; 0 \;\; 0 \;\; 0 \;\; 0 \;\; r_8 \;\; 0 \;\; 0 \;\; 0 \;\; s_8 \;\; 0 \;\; 0 \;\; 0 \;\; t_8\}^T \quad (27)$$

A formal solution of Eq. (24) is given by:

$$\mathbf{Z} = \mathbf{e}^{\mathbf{T}x}\mathbf{K} + \int_0^x \mathbf{e}^{-\mathbf{T}\xi}\mathbf{F}(\xi)d\xi \tag{28}$$

where $\mathbf{K}$ is a vector which can be solved from the BCs at $x = \pm a/2$ and $\mathbf{e}^{\mathbf{Tx}}$ is of the form:

$$\mathbf{e}^{\mathbf{Tx}} = \mathbf{E}\begin{bmatrix} e^{\lambda_1 x} & & 0 \\ & \ddots & \\ 0 & & e^{\lambda_{14} x} \end{bmatrix}\mathbf{E}^{-1} \tag{29}$$

where $\boldsymbol{\lambda}$ and $\mathbf{E}$ are the eigenvalues and columns of eigenvectors, respectively, associated with matrix $\mathbf{T}$. The BCs expressed in terms of displacement variables are described by:

Clamped (C):

$$U = V = \frac{\partial V}{\partial x} = W_b = \frac{\partial W_b}{\partial x} = W_s = \frac{\partial W_s}{\partial x} = 0 \tag{30}$$

Simply supported (S):

$$\begin{aligned}
& U = V = \frac{\partial V}{\partial x} = W_b = W_s \\
& = B_{11}\frac{\partial U_n}{\partial x} - \beta B_{12}V_n - D_{11}\frac{\partial^2 W_{bn}}{\partial x^2} + \beta^2 D_{12}W_{bn} - D_{11}^s\frac{\partial^2 W_{sn}}{\partial x^2} + \beta^2 D_{12}^s W_{sn} \\
& -\beta^2 A_m W_{bn} - \frac{1}{2}\beta^2\left(A_m + B_m\right)W_{sn} - A_m\frac{\partial^2 W_{bn}}{\partial x^2} - \frac{1}{2}\left(A_m + B_m\right)\frac{\partial^2 W_{sn}}{\partial x^2} \\
& = B_{11}\frac{\partial U_n}{\partial x} - \beta B_{12}V_n + \beta^2\left(D_{12} - A_m\right)W_{bn} - \left(D_{11} + A_m\right)\frac{\partial^2 W_{bn}}{\partial x^2} \\
& +\beta^2\left[D_{12}^s - \frac{1}{2}\left(A_m + B_m\right)\right]W_{sn} - \left[D_{11}^s + \frac{1}{2}\left(A_m + B_m\right)\right]\frac{\partial^2 W_{sn}}{\partial x^2}
\end{aligned} \tag{31}$$

Free (F):

$$\begin{aligned}
& A_{11}\frac{\partial U_n}{\partial x} - \beta A_{12}V_x + \beta^2 B_{12}W_{bx} - B_{11}\frac{\partial^2 W_{bn}}{\partial x^2} + \beta^2 B_{12}^s W_{sx} - B_{11}^s\frac{\partial^2 W_{sn}}{\partial x^2} \\
& = \left(\beta A_{66} - \frac{1}{4}\beta^3 A_m\right)U_x + \frac{1}{4}\beta A_m\frac{\partial^2 U_n}{\partial x^2} + \left(A_{66} + \frac{1}{4}\beta^2 A_m\right)\frac{\partial V_n}{\partial x} - \frac{1}{4}A_m\frac{\partial^3 V_n}{\partial x^3} \\
& -2\beta B_{66}\frac{\partial W_{bn}}{\partial x} - 2\beta B_{66}^s\frac{\partial W_{sn}}{\partial x}
\end{aligned}$$

$$=-\frac{1}{2}\beta A_m\frac{\partial U_n}{\partial x}+\frac{1}{2}A_m\frac{\partial^2 V_n}{\partial x^2}-\frac{1}{2}\beta H_m W_{sx}$$

$$\begin{aligned}&=B_{11}\frac{\partial U_n}{\partial x}-\beta B_{12}V_n-D_{11}\frac{\partial^2 W_{bn}}{\partial x^2}+\beta^2 D_{12}W_{bn}-D_{11}^s\frac{\partial^2 W_{sn}}{\partial x^2}+\beta^2 D_{12}^s W_{sn}\\&-\beta^2 A_m W_{bn}-\frac{1}{2}\beta^2\left(A_m+B_m\right)W_{sn}-A_m\frac{\partial^2 W_{bn}}{\partial x^2}-\frac{1}{2}\left(A_m+B_m\right)\frac{\partial^2 W_{sn}}{\partial x^2}\end{aligned}$$

$$\begin{aligned}&=\left(-2\beta^2 B_{66}+\omega^2 I_1+B_{11}a_1\right)U_x+\left[-\beta\left(B_{12}+2B_{66}\right)+B_{11}a_2\right]\frac{\partial V_n}{\partial x}+B_{11}a_3\frac{\partial^3 V_n}{\partial x^3}\\&+\left[\beta^2\left(D_{12}+4D_{66}+A_m\right)+\left(-\omega^2 I_2+P_x^0+P_{xy}^0\right)+B_{11}a_4\right]\frac{\partial W_{bn}}{\partial x}+\left[-\left(D_{11}+A_m\right)+B_{11}a_5\right]\frac{\partial^3 W_{bn}}{\partial x^3}\\&+\left\{\beta^2\left[D_{12}^s+4D_{66}^s+\frac{1}{2}\left(A_m+B_m\right)\right]+\left(-\omega^2 J_2+P_x^0+P_{xy}^0\right)+B_{11}a_6\right\}\frac{\partial W_{sn}}{\partial x}\\&+\left[-D_{11}^s-\frac{1}{2}\left(A_m+B_m\right)+B_{11}a_7\right]\frac{\partial^3 W_{sn}}{\partial x^3}\end{aligned}$$

$$\begin{aligned}&=B_{11}\frac{\partial U_n}{\partial x}-\beta B_{12}V_n+\beta^2\left(D_{12}-A_m\right)W_{bn}-\left(D_{11}+A_m\right)\frac{\partial^2 W_{bn}}{\partial x^2}\\&+\beta^2\left[D_{12}^s-\frac{1}{2}\left(A_m+B_m\right)\right]W_{sn}-\left[D_{11}^s+\frac{1}{2}\left(A_m+B_m\right)\right]\frac{\partial^2 W_{sn}}{\partial x^2}\end{aligned}$$

$$\begin{aligned}&=\left(-2\beta^2 B_{66}^s+\omega^2 J_1+B_{11}^s a_1\right)U_n+\left[-\beta\left(B_{12}^s+2B_{66}^s\right)+B_{11}^s a_2\right]\frac{\partial V_n}{\partial x}+B_{11}^s a_3\frac{\partial^3 V_n}{\partial x^3}\\&+\left[\left(-\omega^2 J_2+P_x^0+P_{xy}^0\right)+\beta^2\left(D_{12}^s+4D_{66}^s+\frac{3}{2}\left(A_m+B_m\right)\right)+B_{11}^s a_4\right]\frac{\partial W_{bn}}{\partial x}\\&+\left(-D_{11}^s-\frac{1}{2}\left(A_m+B_m\right)+B_{11}^s a_5\right)\frac{\partial^3 W_{bn}}{\partial x^3}\\&+\left\{\left(-\omega^2 K_2+P_x^0+P_{xy}^0\right)+A_{55}^s+\frac{1}{4}H_m+\beta^2\left[H_{12}+4H_{66}+\frac{3}{4}\left(A_m+2B_m+C_m\right)\right]+B_{11}^s a_6\right\}\frac{\partial W_{sn}}{\partial x}\\&+\left[-H_{11}-\frac{1}{4}\left(A_m+2B_m+C_m\right)+B_{11}^s a_7\right]\frac{\partial^3 W_{sn}}{\partial x^3}\end{aligned}\tag{32}$$

3.1. Vibration and buckling analysis

As the force vector is vanished in the vibration and buckling analysis, the general solution in Eq. (28) becomes:

$$\mathbf{Z}=\mathbf{e}^{\mathbf{T}x}\mathbf{K}\tag{33}$$

By substituting Eq. (33) into Eqs. (30)-(32) with the required BCs, a system of equations is obtained as:

$$\boldsymbol{\alpha}\mathbf{e}^{\mathbf{T}x}\mathbf{K} = \mathbf{0} \tag{34}$$

where $\boldsymbol{\alpha}$ comes from the coefficients in Eqs. (30)-(32) for the appropriate BCs at $x = \pm a/2$. The natural frequencies ω_n or the buckling loads of the n^{th} mode can be obtained by setting $\left|\boldsymbol{\alpha}\mathbf{e}^{\mathbf{T}x}\right| = 0$. It is noticeable that the iteration procedure [61] is used to calculate the natural frequencies/ buckling loads. The mode shapes are plotted by solving for $\mathbf{K}$ from Eq. (34) based on the singular value decomposition and calculating the displacement components afterward.

3.2. *Static analysis*

The solutions for each value of n, which corresponds to the number of half-sine waves in y-direction can be obtained by substituting Eq. (28) into the appropriate BCs at $x = \pm a/2$. The displacements are then summed up using Eq. (21) regarding the Fourier series form.

4. Numerical examples

In this section, numerical results are presented for the verification and parametric study of the present analytical solution. Unless mentioned otherwise, the material properties are used for metal (Al), $E_m=70GPa$, $\rho_m=2700kg/m^3$, $\nu_m=0.3$ and for ceramic (Al_2O_3), $E_c=380GPa$, $\rho_c=3800kg/m^3$, $\nu_c=0.3$ and the material length scale parameter is assumed $l=17.6\mu m$ based on literature. By using normalized quantities without the inclusion of couple stresses in the strain energy, the displacements, stresses, natural frequencies and critical buckling loads remain constants regardless the material length scale ratio *(h/l)* as long as the distributed load *(q)*, slenderness ratio *(a/h)* and material properties *(E, ν)* are unchanged. Their variations under the MCST demonstrate the size effects in structural behaviours of microplates. The following non-dimensional quantities are used through the paper.

Displacement: $$\bar{w} = \frac{10E_c h^3}{q_0 a^4} u_z\left(0, \frac{b}{2}\right) \tag{35}$$

Stress: $$\bar{\sigma}_{xx} = \frac{h\sigma_{xx}}{aq_0};\ \bar{\sigma}_{xz} = \frac{h\sigma_{xz}}{aq_0} \tag{36}$$

Natural frequency:

$$\hat{\omega} = \frac{\omega a^2}{h}\sqrt{\frac{\rho_c}{E_c}} \tag{37}$$

Buckling load:

$$\bar{P}_{cr} = P_{cr}\frac{a^2}{E_0 h^3} \tag{38}$$

4.1. Verification

a. Static analysis

The verification is firstly carried out for macroplates for various BCs and then simply-supported microplates under uniform loads. Non-dimensional deflection $\bar{w}$ for Al/Al_2O_3 plates for various combinations of clamped (C), simply supported (S) and free (F) are presented in Table 1. For convenience, four-letter abbreviations are used to specify these combinations of boundaries. For example, SCSC plates are referred to the plate having two opposite simply supported edges and two other clamped ones. The present results agree well with those using the finite element method [62] and Levy solution [63] for all BCs and slenderness ratios. Table 2 presents the next verification is carried out for simply-supported Al/Al_2O_3 microplates. A very good agreement between the present results and those from the Navier's solutions, which were based on the FSDT [34] and a refined four-variable shear deformation plate theory (RFVPT) [64], can be observed.

b. Vibration and buckling analysis

Regarding the vibration behaviour, the first four natural frequencies of FG macroplates under various BCs are compared with those from the literature. In Tables 3 and 4, the present results are in excellent agreement with those published by Thai and Choi [65] using the state-space based Levy method for the HSDT. However, the obtained results are slightly higher than those reported by Hosseini-Hashemi et al. [66] using another Levy method. The difference between the present solutions and those reported in [66] is due to the increase of strain energy as a result of the higher-order shear components. The next comparison between the present fundamental frequencies of homogeneous microplates under various BCs and those from Jomehzadeh et al. [67] is depicted in Fig. 2. The material properties analysed in this example are $E=1.44GPa$, $\rho=1.22\times 10^3 kg/m^3$, $\nu=0.38$, $a=b=10mm$. Excellent agreement can be observed for all the material length scale ratios and BCs. Further verification is presented in Table 5 for Mat_1/Mat_2 microplate with the material properties being $E_1=14.4GPa$, $\rho_1=12.2\times 10^3 kg/m^3$, $\nu_1=0.38$ and $E_2=1.44GPa$, $\rho_2=1.22\times 10^3 kg/m^3$, $\nu_2=0.38$, respectively. Again, excellent agreement is observed for the first two modes reported by Thai and Choi [34]. The present HSDT model provides slightly higher natural frequencies compared to the FSDT but smaller values in comparison with the CPT, which neglects the shear deformation effects.

The comparison for the buckling behaviour of FG plates is also carried out in this section. Table 6 presents the non-dimensional buckling loads of Al/Al_2O_3 under the biaxial loads. The present results are nearly the same with those reported by Thai and Uy [68], which are obtained by the Levy solution and neutral axis concept. Further comparison is presented in Table 7 for the size effect in buckling behaviour of Mat_1/Mat_2 plates under biaxial and uniaxial loads. Very good agreement is seen for both thick and thin simply-supported plates.

4.2. Parametric study

a. Static analysis

The deflections and stresses of FG-sandwich ceramic-core microplates with *(1-1-1)* scheme under several BCs are demonstrated in Figs. 3 and 4. For both SCSC and SCSF, the non-dimensional deflection decreases significantly as the thickness reaches to the material length scale parameter. Similarly, the normal and shear stresses are also smaller in micro scales. This is due to the inclusion of couple stress and the corresponding curvatures in the strain energy.

Deflections of various FG-sandwich SCSC microplates with ceramic core and FG-core are presented in Fig. 5. For both types of sandwich plates, the increase of power-law index, which results in the more prominent volume of metal, leads to the increase of deflection. It is understandable as the Young's modulus of metal is smaller than that of ceramic. This can be seen more clearly in the ceramic-core plates, the smallest deflection is obtained as $p=0$, and mount up with the higher power-law indices. The deflection curve is always highest for the thin core *(2-1-2)* and lowest for the thick core *(1-8-1)*. For the FG-core plates, there are changes in the deflection for different schemes as p goes up. The shift approximately occurs at $p=1$ for symmetric geometries and at $p=2$ for asymmetric geometries. The benchmark results for the size-dependent bending behaviour of FG-sandwich plates are presented in Tables 8 and 9 under various BCs.

b. Vibration and buckling analysis

The vibration and buckling behaviours of FG/FG-sandwich plates are presented in this section. The size effect on the natural frequencies of FG plates is presented in Fig. 6. As can be seen for the SCSC plates, the inclusion of couple stress results in a significant increase of frequencies for the small-scale plates, i.e. $h/l<10$. This effect is less important as the thickness of plates is up to $h/l=20$ for all the values of power-law index. By consideration the plates with the thickness the same with material length parameter $(h=l)$ under various BCs, the order of frequencies coincides with the stiffness of BCs, i.e. highest for SCSC and lowest for SFSF. Further investigation for the sandwich microplates is presented in Fig. 7. Opposite to the bending behaviour, the increase of p results in the lower natural frequencies in ceramic-core plates, except for *1-8-1* scheme. It is worth noting that, the natural frequencies are determined by both the Young's modulus and mass density. The increase of metal volume fraction is equivalent to the lower stiffness and lower mass. These factors lead to the decrease of natural frequencies when the ceramic-core is thin, where the Young's modulus contributes more effect. However, for the plates with very thick ceramic core (*1-8-1* scheme), where the stiffness is concentrated near the neutral axis, the decrease of mass is prominent involving the frequencies. Therefore, the increase of p in this case results in a slight escalation of frequencies. For the FG-core plates, the natural frequencies also depend on the relative thickness of the core. As the core is thick enough, i.e. *1-8-1*, *1-2-1* and *2-2-1* plates, the behaviour of these sandwich plates is similar to that of FG plates. In the thin core plates, the increase of metal in the core does not affect the stiffness much while the decrease of mass slightly improves the frequencies. The benchmark results of natural frequencies are presented for some FG-sandwich plates with different slenderness ratios, power-law indices and BCs in Tables 10 and 11. Several mode shapes of FG microplates with SCSC and SFSF boundary conditions are then illustrated in Figs. 8 and 9.

Finally, the critical buckling loads of microplates with various BCs under axial loads are investigated. The size dependent effect on buckling behaviours is presented in Tables 12 and 13 for various FG-core and ceramic-core plates. As expected, the critical buckling loads always decrease with an increase of metal volume fraction for all the schemes (Fig. 10). It is worth nothing that, they only depend on the stiffness; therefore, their variations are more significant in thicker FG layers.

5. Conclusions

In this paper, closed-form solutions have been developed to study the static, free vibration and buckling behaviours of FG sandwich microplates. Governing equations are derived from the variational principle based on the framework of the MCST and a refined plate theory. Utilising the state space approach, the deflection, natural frequencies and critical buckling loads of the FG-sandwich microplates with simply supports at two opposite edges and various BCs for the others are analysed analytically. Utilising the MCST, the behaviours of structures ranged from micro- to macro-scales can be analysed in a unified manner with the material length scale parameter l. The present method is found to be appropriate for the plate thickness ranged from l to any higher values. The solutions for those plates thickened up to $20l$ can be considered as the results for macro-scale ones. The proposed solutions can be obtained with any length scale parameters. This paper also generates the benchmark results for FG and FG-sandwich micro-plates with various configurations, which can be useful in the future reference.

References

[1] Koizumi M. FGM activities in Japan. Composites Part B. 1997;28B:1-4.
[2] Tobioka M. ACE COAT AC 15 aluminum oxide coated cutting tool for highly efficient machining. Technical Report "Sumitomodenki". 1989;135:190-6.
[3] Gasik MM. Functionally graded materials: bulk processing techniques. International Journal of Materials and Product Technology. 2010;39:20-9.
[4] Miyamoto Y, Kaysser W, Rabin B, Kawasaki A, Ford R. Functionally graded materials: design, processing and applications: Springer Science & Business Media; 2013.
[5] Kieback B, Neubrand A, Riedel H, Processing techniques for functionally graded materials, Materials Science and Engineering: A. 2003; 362 (1–2), 81-106
[6] Singh S, Singh R. Effect of process parameters on micro hardness of Al–Al2O3 composite prepared using an alternative reinforced pattern in fused deposition modelling assisted investment casting. Robotics and Computer-Integrated Manufacturing. 2016;37:162-9.
[7] Yan W, Ge W, Smith J, Lin S, Kafka OL, Lin F, et al. Multi-scale modeling of electron beam melting of functionally graded materials. Acta Materialia. 2016;115:403-12.
[8] Zygmuntowicz J, Miazga A, Wiecinska P, Kaszuwara W, Konopka K, Szafran M. Combined centrifugal-slip casting method used for preparation the Al2O3 -Ni functionally graded composites. Composites Part B: Engineering. 2018;141:158-63.
[9] Fleck NA, Muller GM, Ashby MF, Hutchinson JW. Strain gradient plasticity: Theory and experiment. Acta Metallurgica et Materialia. 1994;42(2):475-87.
[10] Stolken JS, Evans AG. A microbend test method for measuring the plasticity length scale. Acta Metall Mater. 1998;46:5109-15.
[11] Lam DCC, Yang F, Chong ACM, Wang J, Tong P. Experiments and theory in strain gradient elasticity. Journal of the Mechanics and Physics of Solids. 2003;51(8):1477-508.
[12] Cosserat E, Cosserat F. Theory of deformable bodies (Translated by D.H. Delphenich). Paris: Sorbonne: Herman and Sons; 1909.
[13] Thai H-T, Vo TP, Nguyen T-K, Kim S-E. A review of continuum mechanics models for size-dependent analysis of beams and plates. Composite Structures. 2017;177:196-219.
[14] Eringen AC. Simple microfluids. International Journal of Engineering Science. 1964;2:205-17.
[15] Eringen AC, Suhubi ES. Nonlinear theory of simple microelastic solid-II. International Journal of Engineering Science. 1964;2:389–404.
[16] Eringen AC. Linear theory of micropolar elasticity Journal of Mathematics and Mechanics. 1966;15(6):909-23.
[17] Eringen AC. Micropolar fluids with stretch. International Journal of Engineering Science. 1969;7:115-27.
[18] Neff P, Forest S. A Geometrically Exact Micromorphic Model for Elastic Metallic Foams Accounting for Affine Microstructure. Modelling, Existence of Minimizers, Identification of Moduli and Computational Results. J Elasticity. 2007;87(2-3):239-76.
[19] Kröner E. Elasticity theory of materials with long range cohesive forces. International Journal of Solids and Structures. 1967;3(5):731-42.
[20] Eringen AC. Linear theory of nonlocal elasticity and dispersion of plane waves. International Journal of Engineering Science. 1972;10(5):425-35.
[21] Eringen AC. Nonlocal polar elastic continua. International Journal of Engineering Science. 1972;10(1):1-16.
[22] Eringen AC, Edelen DGB. On nonlocal elasticity. International Journal of Engineering Science. 1972;10(3):233-48.
[23] Mindlin RD. Micro-structure in linear elasticity. Archives of Rational Mechanics and Analysis. 1964;16:51-78.

[24] Mindlin RD. Second gradient of strain and surface tension in linear elasticity. Archive for Rational Mechanics and Analysis. 1965;16:51-78.
[25] Toupin RA. Elastic materials with couple stresses. Archives of Rational of Mechanical and Analysis. 1962;11:385–414.
[26] Toupin RA. Theory of elasticity with couple stresses. Archives of Rational Mechanics and Analysis. 1964;17:85-112.
[27] Mindlin RD, Tiersten HF. Effects of couple-stresses in linear elasticity. Archives of Rational Mechanics and Analysis. 1962;11:415–48.
[28] Koiter WT. Couple stresses in the theory of elasticity. I and II Proc K Ned Akad Wet 1964;B(67):17-44.
[29] Yang F, Chong ACM, Lam DCC, Tong P. Couple stress based strain gradient theory for elasticity. International Journal of Solids and Structures. 2002;39:2731–43.
[30] Munch I, Neff P, Madeo A, Ghiba I-D. The modified indeterminate couple stress model- Why Yang et al. arguments motivating a symmetric couple stress tensor contain a gap and why the couple stress tensor may be chosen symmetric nevertheless. 2017.
[31] Asghari M, Taati E. A size-dependent model for functionally graded micro-plates for mechanical analyses. Journal of Vibration and Control. 2012;19(11):1614-32.
[32] Taati E. Analytical solutions for the size dependent buckling and postbuckling behavior of functionally graded micro-plates. International Journal of Engineering Science. 2016;100:45-60.
[33] Ke LL, Yang J, Kitipornchai S, Bradford MA. Bending, buckling and vibration of size-dependent functionally graded annular microplates. Composite Structures. 2012;94(11):3250-7.
[34] Thai H-T, Choi D-H. Size-dependent functionally graded Kirchhoff and Mindlin plate models based on a modified couple stress theory. Composite Structures. 2013;95:142-53.
[35] Jung W-Y, Han S-C, Park W-T. A modified couple stress theory for buckling analysis of S-FGM nanoplates embedded in Pasternak elastic medium. Composites Part B: Engineering. 2014;60:746-56.
[36] Jung W-Y, Park W-T, Han S-C. Bending and vibration analysis of S-FGM microplates embedded in Pasternak elastic medium using the modified couple stress theory. International Journal of Mechanical Sciences. 2014;87:150-62.
[37] Ansari R, Faghih Shojaei M, Mohammadi V, Gholami R, Darabi MA. Nonlinear vibrations of functionally graded Mindlin microplates based on the modified couple stress theory. Composite Structures. 2014;114:124-34.
[38] Ansari R, Gholami R, Faghih Shojaei M, Mohammadi V, Darabi MA. Size-dependent nonlinear bending and postbuckling of functionally graded Mindlin rectangular microplates considering the physical neutral plane position. Composite Structures. 2015;127:87-98.
[39] Li D, Deng Z, Xiao H. Thermomechanical bending analysis of functionally graded sandwich plates using four-variable refined plate theory. Composites Part B: Engineering. 2016;106:107-19.
[40] Gupta A, Talha M, Singh BN. Vibration characteristics of functionally graded material plate with various boundary constraints using higher order shear deformation theory. Composites Part B: Engineering. 2016;94:64-74.
[41] Karamanli, A and Vo, TP. Size dependent bending analysis of two directional functionally graded microbeams via a quasi-3D theory and finite element method. Composites Part B: Engineering. 2018; 144, 171-183.
[42] Phung-Van P, Ferreira AJM, Nguyen-Xuan H, Abdel Wahab M. An isogeometric approach for size-dependent geometrically nonlinear transient analysis of functionally graded nanoplates. Composites Part B: Engineering. 2017;118:125-34.
[43] Farzam-Rad SA, Hassani B, Karamodin A. Isogeometric analysis of functionally graded plates using a new quasi-3D shear deformation theory based on physical neutral surface. Composites Part B: Engineering. 2017;108:174-89.

[44] Demirbas MD. Thermal stress analysis of functionally graded plates with temperature-dependent material properties using theory of elasticity. Composites Part B: Engineering. 2017;131:100-24.
[45] Thai H-T, Kim S-E. A size-dependent functionally graded Reddy plate model based on a modified couple stress theory. Composites Part B: Engineering. 2013;45(1):1636-45.
[46] Eshraghi I, Dag S, Soltani N. Consideration of spatial variation of the length scale parameter in static and dynamic analyses of functionally graded annular and circular micro-plates. Composites Part B: Engineering. 2015;78:338-48.
[47] Thai H-T, Vo TP. A size-dependent functionally graded sinusoidal plate model based on a modified couple stress theory. Composite Structures. 2013;96:376-83.
[48] He L, Lou J, Zhang E, Wang Y, Bai Y. A size-dependent four variable refined plate model for functionally graded microplates based on modified couple stress theory. Composite Structures. 2015;130:107-15.
[49] Lou J, He L, Du J. A unified higher order plate theory for functionally graded microplates based on the modified couple stress theory. Composite Structures. 2015;133:1036-47.
[50] Lei J, He Y, Zhang B, Liu D, Shen L, Guo S. A size-dependent FG micro-plate model incorporating higher-order shear and normal deformation effects based on a modified couple stress theory. International Journal of Mechanical Sciences. 2015;104:8-23.
[51] Nguyen HX, Nguyen TN, Abdel-Wahab M, Bordas SPA, Nguyen-Xuan H, Vo TP. A refined quasi-3D isogeometric analysis for functionally graded microplates based on the modified couple stress theory. Computer Methods in Applied Mechanics and Engineering. 2017;313:904-40.
[52] Trinh LC, Vo TP, Thai H-T, Mantari JL. Size-dependent behaviour of functionally graded sandwich microplates under mechanical and thermal loads. Composites Part B: Engineering. 2017;124:218-41.
[53] Mirsalehi M, Azhari M, Amoushahi H. Stability of thin FGM microplate subjected to mechanical and thermal loading based on the modified couple stress theory and spline finite strip method. Aerospace Science and Technology. 2015;47:356-66.
[54] Ashoori AR, Sadough Vanini SA. Thermal buckling of annular microstructure-dependent functionally graded material plates resting on an elastic medium. Composites Part B: Engineering. 2016;87:245-55.
[55] Eshraghi I, Dag S, Soltani N. Bending and free vibrations of functionally graded annular and circular micro-plates under thermal loading. Composite Structures. 2016;137:196-207.
[56] Thai H-T, Vo TP. Bending and free vibration of functionally graded beams using various higher-order shear deformation beam theories. International Journal of Mechanical Sciences. 2012;62(1):57-66.
[57] Birman V, Kardomateas GA. Review of current trends in research and applications of sandwich structures. Composites Part B: Engineering. 2018;142:221-40.
[58] Nguyen V-H, Nguyen T-K, Thai H-T, Vo TP. A new inverse trigonometric shear deformation theory for isotropic and functionally graded sandwich plates. Composites Part B: Engineering. 2014;66:233-46.
[59] Nguyen T-K, Nguyen V-H, Chau-Dinh T, Vo TP, Nguyen-Xuan H. Static and vibration analysis of isotropic and functionally graded sandwich plates using an edge-based MITC3 finite elements. Composites Part B: Engineering. 2016;107:162-73.
[60] Thai HT, Kim SE. Analytical solution of a two variable refined plate theory for bending analysis of orthotropic Levy-type plates. International Journal of Mechanical Sciences. 2012;54(1):269-76.
[61] Thai HT, Kim SE. Levy-type solution for free vibration analysis of orthotropic plates based on two variable refined plate theory. Applied Mathematical Modelling. 2012;36(8):3870-82.
[62] Thai H-T, Choi D-H. Finite element formulation of various four unknown shear deformation theories for functionally graded plates. Finite Elements in Analysis and Design. 2013;75:50-61.

[63] Demirhan PA, Taskin V. Levy solution for bending analysis of functionally graded sandwich plates based on four variable plate theory. Composite Structures. 2017;177:80-95.
[64] Abazid MA, Sobhy M. Thermo-electro-mechanical bending of FG piezoelectric microplates on Pasternak foundation based on a four-variable plate model and the modified couple stress theory. Microsystem Technologies. 2017.
[65] Thai HT, Choi DH. Levy solution for free vibration analysis of functionally graded plates based on a refined plate theory. Ksce J Civ Eng. 2014;18(6):1813-24.
[66] Hosseini-Hashemi S, Fadaee M, Atashipour SR. A new exact analytical approach for free vibration of Reissner–Mindlin functionally graded rectangular plates. International Journal of Mechanical Sciences. 2011;53(1):11-22.
[67] Jomehzadeh E, Noori HR, Saidi AR. The size-dependent vibration analysis of micro-plates based on a modified couple stress theory. Physica E: Low-dimensional Systems and Nanostructures. 2011;43(4):877-83.
[68] Thai HT, Uy B. Levy solution for buckling analysis of functionally graded plates based on a refined plate theory. P I Mech Eng C-J Mec. 2013;227(12):2649-64.

Table 1: Non-dimensional deflections of Al/Al_2O_3 plates under various BCs.

a/h	p	Theory	SCSC	SCSS	SSSS	SCSF	SSSF	SFSF
5	0	HSDT [62]	0.309	0.402	0.538	0.758	0.999	1.615
		HSDT [63]	0.299	0.395	0.535	0.739	0.987	1.586
		Present HSDT	0.322	0.418	0.559	0.762	1.011	1.610
	0.5	HSDT [62]	0.458	0.602	0.812	1.143	1.515	2.457
		HSDT [63]	0.444	0.592	0.809	1.117	1.500	2.417
		Present HSDT	0.478	0.623	0.832	1.151	1.527	2.452
	1	HSDT [62]	0.586	0.773	1.049	1.473	1.959	3.176
		HSDT [63]	0.571	0.763	1.045	1.444	1.942	3.132
		Present HSDT	0.614	0.798	1.057	1.487	1.964	3.177
	2	HSDT [62]	0.761	1.003	1.357	1.900	2.525	4.085
		HSDT [63]	0.746	0.993	1.354	1.869	2.508	4.038
		Present HSDT	0.802	1.032	1.348	1.927	2.521	4.098
	5	HSDT [62]	0.990	1.277	1.697	2.369	3.109	4.991
		HSDT [63]	0.971	1.264	1.693	2.330	3.087	4.932
		Present HSDT	1.050	1.325	1.707	2.410	3.121	5.015
	10	HSDT [62]	1.137	1.452	1.913	2.670	3.481	5.573
		HSDT [63]	1.112	1.435	1.906	2.620	3.452	5.495
		Present HSDT	1.204	1.516	1.957	2.714	3.518	5.592
20	0	HSDT [62]	0.226	0.317	0.452	0.646	0.885	1.469
		HSDT [63]	0.215	0.310	0.449	0.626	0.874	1.440
		Present HSDT	0.227	0.322	0.461	0.639	0.886	1.452
	0.5	HSDT [62]	0.345	0.487	0.696	0.992	1.362	2.259
		HSDT [63]	0.331	0.477	0.692	0.965	1.346	2.219
		Present HSDT	0.348	0.492	0.700	0.983	1.358	2.238
	1	HSDT [62]	0.445	0.630	0.903	1.284	1.767	2.929
		HSDT [63]	0.430	0.620	0.900	1.254	1.750	2.885
		Present HSDT	0.452	0.635	0.892	1.278	1.753	2.910
	2	HSDT [62]	0.567	0.806	1.157	1.640	2.262	3.745
		HSDT [63]	0.552	0.795	1.154	1.609	2.244	3.699
		Present HSDT	0.581	0.807	1.121	1.640	2.230	3.731
	5	HSDT [62]	0.678	0.960	1.375	1.949	2.684	4.443
		HSDT [63]	0.658	0.946	1.370	1.910	2.662	4.384
		Present HSDT	0.693	0.964	1.341	1.947	2.652	4.423
	10	HSDT [62]	0.752	1.060	1.514	2.153	2.956	4.896
		HSDT [63]	0.725	1.042	1.507	2.101	2.926	4.818
		Present HSDT	0.765	1.071	1.507	2.142	2.939	4.861

Table 2: Non-dimensional deflections of simply-supported Al/Al_2O_3 microplates under uniform load.

a/h	l/h	p = 0			p = 1			p = 10		
		FSDT [34]	RFVPT [64]	Present HSDT	FSDT [34]	RFVPT [64]	Present HSDT	FSDT [34]	RFVPT [64]	Present HSDT
5	0.0	0.515	0.510	0.538	1.154	1.144	1.155	2.627	2.826	2.853
	0.2	0.448	0.432	0.467	0.969	0.940	0.974	2.313	2.357	2.416
	0.4	0.325	0.297	0.335	0.660	0.612	0.668	1.714	1.590	1.689
	0.6	0.227	0.196	0.228	0.440	0.387	0.440	1.216	1.043	1.138
	0.8	0.163	0.133	0.158	0.307	0.256	0.298	0.884	0.708	0.785
	1.0	0.123	0.094	0.113	0.228	0.178	0.211	0.671	0.503	0.563
10	0.0	0.442	0.440	0.455	1.021	1.018	1.004	2.225	2.276	2.223
	0.2	0.384	0.381	0.396	0.857	0.850	0.848	1.959	1.972	1.943
	0.4	0.278	0.271	0.285	0.580	0.568	0.580	1.446	1.416	1.421
	0.6	0.191	0.183	0.195	0.379	0.366	0.381	1.012	0.968	0.987
	0.8	0.134	0.126	0.135	0.257	0.244	0.257	0.717	0.672	0.693
	1.0	0.097	0.090	0.096	0.184	0.171	0.181	0.526	0.483	0.501
20	0.0	0.423	0.423	0.435	0.987	0.987	0.966	2.124	2.137	2.065
	0.2	0.368	0.367	0.378	0.829	0.827	0.816	1.871	1.874	1.823
	0.4	0.266	0.264	0.272	0.560	0.557	0.558	1.378	1.371	1.353
	0.6	0.181	0.180	0.186	0.364	0.360	0.365	0.959	0.948	0.949
	0.8	0.126	0.124	0.129	0.245	0.242	0.247	0.674	0.663	0.669
	1.0	0.091	0.089	0.092	0.172	0.169	0.174	0.489	0.478	0.485

Table 3: The first four natural frequencies of Al/Al_2O_3 plates with SCSC and SCSS boundary conditions (a/h=5).

BCs	Mode	Theory	p						
			0	0.5	1	2	5	8	10
SCSC	1	FSDT [66]	6.766	5.841	5.304	4.803	4.413	4.260	4.187
		HSDT [65]	7.110	6.132	5.551	4.992	4.513	-	4.285
		Present HSDT	7.110	6.133	5.552	4.993	4.514	4.351	4.286
	2	FSDT [66]	12.060	10.420	9.456	8.547	7.833	7.561	7.431
		Present HSDT	12.400	10.731	9.715	8.709	7.800	7.498	7.385
	3	FSDT [66]	13.501	11.758	10.712	9.676	8.755	8.396	8.235
		Present HSDT	14.319	12.480	11.331	10.132	8.930	8.531	8.393
	4	FSDT [66]	17.718	15.423	14.040	12.670	11.473	11.011	10.802
		Present HSDT	18.567	16.202	14.709	13.135	11.537	11.011	10.832
SCSS	1	FSDT [66]	5.963	5.119	4.636	4.200	3.892	3.775	3.715
		HSDT [65]	6.117	5.250	4.744	4.275	3.910	-	3.732
		Present HSDT	6.117	5.252	4.748	4.281	3.915	3.789	3.735
	2	FSDT [66]	11.786	10.165	9.217	8.331	7.657	7.401	7.277
		Present HSDT	11.935	10.312	9.330	8.370	7.525	7.243	7.136
	3	FSDT [66]	12.543	10.865	9.874	8.924	8.144	7.844	7.703
		Present HSDT	12.904	11.202	10.164	9.117	8.119	7.782	7.658
	4	FSDT [66]	17.199	14.930	13.571	12.249	11.142	10.717	10.521
		Present HSDT	19.133	17.156	15.741	14.059	12.326	11.569	11.275

Table 4: The first four natural frequencies of Al/ZrO_2 plates with SCSF, SSSF and SFSF boundary conditions (a/h=5).

BCs	Mode	Theory	p						
			0	0.5	1	2	5	8	10
SCSF	1	FSDT [66]	3.438	3.253	3.180	3.165	3.209	3.206	3.194
		HSDT [65]	3.528	3.337	3.260	3.239	3.276	3.274	3.264
		Present HSDT	3.528	3.337	3.260	3.239	3.277	3.275	3.265
	2	FSDT [66]	7.794	7.417	7.255	7.189	7.218	7.192	7.163
		Present HSDT	8.214	7.814	7.633	7.539	7.534	7.516	7.497
	3	FSDT [66]	9.954	9.471	9.265	9.183	9.224	9.190	9.153
		Present HSDT	10.077	9.601	9.378	9.250	9.215	9.188	9.166
	4	FSDT [66]	13.534	12.921	12.643	12.502	12.489	12.426	12.373
		Present HSDT	14.012	13.395	13.083	12.859	12.722	12.671	12.643
SSSF	1	FSDT [66]	3.438	3.253	3.180	3.165	3.209	3.206	3.194
		HSDT [65]	3.278	3.099	3.027	3.010	3.048	3.047	3.038
		Present HSDT	3.278	3.101	3.032	3.016	3.053	3.050	3.041
	2	FSDT [66]	7.794	7.417	7.255	7.189	7.218	7.192	7.163
		Present HSDT	7.183	6.821	6.666	6.600	6.624	6.612	6.594
	3	FSDT [66]	9.954	9.471	9.265	9.183	9.224	9.190	9.153
		Present HSDT	9.985	9.513	9.293	9.167	9.135	9.109	9.086
	4	FSDT [66]	13.534	12.921	12.643	12.502	12.489	12.426	12.373
		Present HSDT	13.413	12.815	12.521	12.321	12.211	12.164	12.135
SFSF	1	FSDT [66]	2.718	2.567	2.510	2.501	2.543	2.542	2.533
		HSDT [65]	2.733	2.582	2.523	2.509	2.545	2.545	2.537
		Present HSDT	2.733	2.582	2.523	2.510	2.545	2.545	2.538
	2	FSDT [66]	4.265	4.038	3.947	3.926	3.976	3.971	3.956
		Present HSDT	4.434	4.196	4.100	4.072	4.116	4.114	4.102
	3	FSDT [66]	8.817	8.377	8.190	8.122	8.177	8.155	8.124
		Present HSDT	9.524	9.069	8.859	8.742	8.719	8.695	8.674
	4	FSDT [66]	9.463	8.998	8.802	8.728	8.775	8.745	8.710
		Present HSDT	11.118	10.598	10.351	10.204	10.156	10.125	10.101

Table 5: Size effect in the first two natural frequencies of simply supported plates.

a/h	l/h	p = 0			p = 1			p = 10		
		CPT [34]	FSDT [34]	Present HSDT	CPT [34]	FSDT [34]	Present HSDT	CPT [34]	FSDT [34]	Present HSDT
First mode										
5	0	5.967	5.387	5.388	5.296	4.874	4.910	6.232	5.582	5.422
	0.2	6.396	5.780	5.781	5.781	5.324	5.349	6.641	5.955	5.875
	0.4	7.537	6.800	6.822	7.038	6.460	6.478	7.740	6.933	7.016
	0.6	9.126	8.160	8.270	8.741	7.930	8.003	9.287	8.252	8.543
	0.8	10.972	9.645	9.948	10.677	9.500	9.733	11.095	9.705	10.269
	1	12.964	11.131	11.759	12.742	11.045	11.549	13.058	11.167	11.965
10	0	6.110	5.930	5.930	5.395	5.270	5.318	6.396	6.190	6.185
	0.2	6.549	6.356	6.357	5.889	5.752	5.795	6.816	6.597	6.621
	0.4	7.717	7.481	7.491	7.170	6.992	7.029	7.943	7.680	7.759
	0.6	9.345	9.026	9.071	8.905	8.648	8.701	9.530	9.183	9.337
	0.8	11.235	10.785	10.905	10.878	10.494	10.606	11.387	10.907	11.169
	1	13.275	12.636	12.884	12.981	12.413	12.637	13.401	12.730	13.150
20	0	6.148	6.100	6.098	5.421	5.388	5.439	6.439	6.384	6.443
	0.2	6.589	6.538	6.538	5.918	5.881	5.931	6.861	6.803	6.869
	0.4	7.765	7.701	7.704	7.204	7.157	7.199	7.997	7.925	8.000
	0.6	9.403	9.316	9.329	8.947	8.878	8.919	9.594	9.499	9.588
	0.8	11.304	11.180	11.215	10.929	10.826	10.879	11.463	11.330	11.444
	1	13.356	13.179	13.251	13.043	12.887	12.970	13.491	13.303	13.458
Second mode										
5	0	14.272	11.672	11.685	12.782	10.791	10.821	14.849	11.993	11.275
	0.2	15.297	12.574	12.673	13.953	11.826	11.907	15.823	12.851	12.564
	0.4	18.025	14.865	15.258	16.987	14.379	14.676	18.441	15.050	15.648
	0.6	21.828	17.806	18.792	21.096	17.549	18.376	22.126	17.906	19.569
	0.8	24.252	20.854	22.401	24.252	20.747	22.310	24.252	20.897	22.352
	1	25.838	23.702	23.722	25.838	23.672	23.699	25.838	23.715	23.687
10	0	15.094	14.089	14.091	13.363	12.646	12.681	15.781	14.646	14.314
	0.2	16.178	15.106	15.150	14.586	13.806	13.863	16.817	15.614	15.491
	0.4	19.063	17.768	17.955	17.758	16.760	16.912	19.599	18.171	18.471
	0.6	23.085	21.365	21.844	22.054	20.638	21.027	23.515	21.661	22.482
	0.8	27.753	25.366	26.341	26.940	24.860	25.699	28.095	25.574	27.068
	1	32.792	29.459	31.185	32.149	29.117	30.676	33.065	29.601	31.991
20	0	15.322	15.032	15.029	13.520	13.319	13.357	16.043	15.711	15.646
	0.2	16.423	16.111	16.124	14.759	14.538	14.584	17.096	16.742	16.745
	0.4	19.352	18.969	19.028	17.968	17.681	17.753	19.924	19.496	19.632
	0.6	23.435	22.915	23.070	22.314	21.899	22.041	23.905	23.338	23.637
	0.8	28.173	27.437	27.757	27.258	26.636	26.919	28.562	27.774	28.291
	1	33.289	32.237	32.813	32.529	31.601	32.119	33.613	32.507	33.326

Table 6: Non-dimensional buckling loads of Al/Al_2O_3 plates under various BCs (a/h=5).

BCs	Theory	p					
		0	0.5	1	2	5	10
SCSC	Present HSDT	13.1426	8.8460	6.8778	5.2642	4.0410	3.5278
	HSDT [68]	13.1425	8.8460	6.8778	5.2642	4.0410	3.5278
SCSS	Present HSDT	10.0551	6.7079	5.2014	3.9994	3.1389	2.7657
	HSDT [68]	10.0551	6.7079	5.2014	3.9994	3.1389	2.7657
SSSS	Present HSDT	8.0106	5.3127	4.1122	3.1716	2.5265	2.2403
	HSDT [68]	8.0105	5.3127	4.1122	3.1716	2.5265	2.2403
SCSF	Present HSDT	4.9706	3.2680	2.5230	1.9546	1.5923	1.4259
	HSDT [68]	4.9706	3.2680	2.5231	1.9547	1.5924	1.4260
SSSF	Present HSDT	4.6270	3.0444	2.3556	1.8304	1.4931	1.3355
	HSDT [68]	4.6270	3.0391	2.3457	1.8182	1.4850	1.3313
SFSF	Present HSDT	4.1391	2.7149	2.0946	1.6247	1.3318	1.1959
	HSDT [68]	4.1391	2.7149	2.0946	1.6247	1.3318	1.1959

Table 7: Size effect in the buckling behaviour of simply supported plates.

a/h	l/h	p = 0			p = 1			p = 10		
		CPT [34]	FSDT [34]	Present HSDT	CPT [34]	FSDT [34]	Present HSDT	CPT [34]	FSDT [34]	Present HSDT
Biaxial buckling ($\gamma_1 = \gamma_2 = -1$)										
5	0	19.226	15.323	15.332	8.215	6.858	6.976	3.836	2.998	2.821
	0.2	22.086	17.615	17.640	9.788	8.172	8.276	4.356	3.408	3.322
	0.4	30.669	24.290	24.553	14.508	11.992	12.128	5.916	4.601	4.761
	0.6	44.972	34.786	36.059	22.375	17.984	18.504	8.517	6.480	7.094
	0.8	64.998	48.292	52.153	33.389	25.665	27.394	12.158	8.902	10.318
	1	90.744	63.891	72.833	47.550	34.498	38.800	16.839	11.704	14.441
10	0	19.226	18.075	18.076	8.215	7.827	7.978	3.836	3.585	3.582
	0.2	22.086	20.761	20.766	9.788	9.324	9.474	4.356	4.071	4.104
	0.4	30.669	28.748	28.835	14.508	13.774	13.936	5.916	5.515	5.635
	0.6	44.972	41.827	42.282	22.375	21.060	21.354	8.517	7.880	8.168
	0.8	64.998	59.666	61.095	33.389	30.993	31.724	12.158	11.107	11.695
	1	90.744	81.827	85.287	47.550	43.327	45.040	16.839	15.115	16.217
20	0	19.226	18.924	18.924	8.215	8.114	8.276	3.836	3.770	3.842
	0.2	22.086	21.739	21.733	9.788	9.668	9.817	4.356	4.281	4.356
	0.4	30.669	30.163	30.177	14.508	14.317	14.457	5.916	5.810	5.903
	0.6	44.972	44.137	44.224	22.375	22.029	22.206	8.517	8.347	8.475
	0.8	64.998	63.566	63.952	33.389	32.752	33.081	12.158	11.875	12.121
	1	90.744	88.316	89.252	47.550	46.411	46.954	16.839	16.368	16.730
Uniaxial buckling ($\gamma_1 = -1$, $\gamma_2 = 0$)										
5	0	38.451	30.646	30.665	16.429	13.715	13.945	7.672	5.996	5.631
	0.2	44.173	35.230	35.279	19.576	16.343	16.544	8.712	6.815	6.637
	0.4	61.337	48.580	49.104	29.016	23.984	24.252	11.833	9.203	9.519
	0.6	89.945	69.571	72.115	44.751	35.968	37.003	17.034	12.961	14.184
	0.8	129.995	96.583	104.305	66.778	51.331	54.782	24.316	17.804	20.632
	1	181.489	127.783	145.671	95.100	68.996	77.597	33.679	23.408	28.878
10	0	38.451	36.149	36.151	16.429	15.655	15.949	7.672	7.171	7.157
	0.2	44.173	41.521	41.533	19.576	18.648	18.939	8.712	8.142	8.203
	0.4	61.337	57.496	57.678	29.016	27.548	27.865	11.833	11.030	11.277
	0.6	89.945	83.654	84.564	44.751	42.119	42.708	17.034	15.761	16.335
	0.8	129.995	119.331	122.191	66.778	61.986	63.447	24.316	22.213	23.390
	1	181.489	163.654	170.573	95.100	86.655	90.081	33.679	30.230	32.434
20	0	38.451	37.849	37.849	16.429	16.228	16.545	7.672	7.540	7.679
	0.2	44.173	43.477	43.466	19.576	19.335	19.650	8.712	8.562	8.712
	0.4	61.337	60.325	60.354	29.016	28.633	28.946	11.833	11.621	11.837
	0.6	89.945	88.274	88.494	44.751	44.058	44.460	17.034	16.695	16.998
	0.8	129.995	127.131	127.904	66.778	65.503	66.162	24.316	23.749	24.179
	1	181.489	176.631	178.583	95.100	92.821	93.987	33.679	32.736	33.460

Table 8: Non-dimensional deflections and stresses of SCSC, SCSS and SSSS (1-1-1) sandwich plates (a/h=5).

Core	BCs	h/l	$\bar{w}(0,b/2)$			$\bar{\sigma}_x(0,b/2,h/2)$			$\bar{\sigma}_y(0,b/2,h/2)$		
			p=0	1	10	p=0	1	10	p=0	1	10
FG	SCSC	1	0.082	0.097	0.114	0.232	0.254	0.281	0.205	0.227	0.251
		2	0.227	0.275	0.325	0.678	0.737	0.792	0.617	0.672	0.724
		4	0.419	0.510	0.605	1.287	1.386	1.448	1.208	1.306	1.373
		∞	0.591	0.722	0.855	1.831	1.958	2.001	1.768	1.908	1.989
	SCSS	1	0.113	0.135	0.159	0.290	0.327	0.369	0.270	0.296	0.327
		2	0.310	0.373	0.440	0.839	0.933	1.023	0.785	0.845	0.902
		4	0.561	0.676	0.791	1.575	1.729	1.834	1.499	1.593	1.654
		∞	0.780	0.937	1.086	2.222	2.416	2.501	2.156	2.280	2.333
	SSSS	1	0.160	0.192	0.228	0.325	0.350	0.380	0.379	0.421	0.470
		2	0.436	0.529	0.626	0.944	1.018	1.088	1.085	1.185	1.282
		4	0.788	0.956	1.115	1.778	1.905	1.979	2.045	2.208	2.312
		∞	1.091	1.317	1.509	2.524	2.691	2.732	2.907	3.114	3.193
Ceramic	SCSC	1	0.055	0.086	0.133	0.205	0.056	0.084	0.180	0.049	0.073
		2	0.146	0.230	0.361	0.539	0.163	0.265	0.486	0.148	0.240
		4	0.246	0.415	0.707	0.902	0.308	0.558	0.846	0.288	0.519
		∞	0.322	0.579	1.083	1.163	0.435	0.876	1.134	0.419	0.832
	SCSS	1	0.077	0.118	0.182	0.242	0.066	0.099	0.239	0.065	0.097
		2	0.197	0.314	0.496	0.629	0.191	0.309	0.634	0.193	0.312
		4	0.326	0.562	0.973	1.044	0.357	0.647	1.081	0.369	0.665
		∞	0.419	0.775	1.485	1.339	0.501	1.013	1.424	0.529	1.057
	SSSS	1	0.108	0.165	0.253	0.297	0.081	0.122	0.327	0.089	0.134
		2	0.273	0.437	0.694	0.763	0.231	0.375	0.852	0.258	0.419
		4	0.443	0.776	1.362	1.253	0.428	0.778	1.424	0.486	0.880
		∞	0.559	1.063	2.075	1.598	0.600	1.215	1.850	0.690	1.387

Table 9: Non-dimensional deflections and stresses of SCSF, SSSF and SFSF (1-1-1) sandwich plates (a/h=5).

Core	BCs	h/l	$\bar{w}(0,b/2)$			$\bar{\sigma}_x(0,b/2,h/2)$			$\bar{\sigma}_y(0,b/2,h/2)$		
			p=0	1	10	p=0	1	10	p=0	1	10
FG	SCSF	1	0.196	0.236	0.284	0.287	0.323	0.359	0.388	0.422	0.467
		2	0.573	0.698	0.831	0.733	0.796	0.854	1.235	1.342	1.447
		4	1.072	1.300	1.510	1.244	1.334	1.382	2.371	2.552	2.659
		∞	1.496	1.805	2.061	1.559	1.668	1.704	3.322	3.556	3.641
	SSSF	1	0.265	0.320	0.384	0.392	0.447	0.507	0.525	0.569	0.627
		2	0.776	0.941	1.115	1.019	1.130	1.235	1.643	1.766	1.889
		4	1.439	1.728	1.989	1.739	1.899	1.997	3.116	3.301	3.399
		∞	1.987	2.364	2.660	2.193	2.380	2.459	4.312	4.525	4.555
	SFSF	1	0.383	0.465	0.564	0.407	0.467	0.530	0.690	0.745	0.824
		2	1.218	1.487	1.780	0.975	1.060	1.135	2.425	2.634	2.854
		4	2.353	2.849	3.284	1.469	1.565	1.595	4.763	5.118	5.313
		∞	3.260	3.910	4.391	1.493	1.594	1.621	6.518	6.943	7.029
Ceramic	SCSF	1	0.135	0.201	0.304	0.230	0.063	0.095	0.361	0.096	0.142
		2	0.362	0.574	0.900	0.561	0.175	0.290	0.996	0.299	0.480
		4	0.598	1.055	1.853	0.843	0.297	0.555	1.655	0.567	1.029
		∞	0.763	1.458	2.857	0.991	0.370	0.747	2.113	0.788	1.588
	SSSF	1	0.184	0.273	0.410	0.305	0.083	0.124	0.493	0.131	0.193
		2	0.492	0.781	1.227	0.748	0.231	0.381	1.358	0.406	0.650
		4	0.804	1.433	2.536	1.123	0.395	0.735	2.238	0.767	1.391
		∞	1.011	1.968	3.901	1.318	0.494	1.001	2.824	1.058	2.140
	SFSF	1	0.269	0.391	0.580	0.310	0.084	0.125	0.673	0.174	0.253
		2	0.774	1.214	1.887	0.729	0.231	0.387	2.005	0.590	0.933
		4	1.283	2.307	4.092	0.951	0.350	0.680	3.325	1.140	2.069
		∞	1.610	3.171	6.332	0.947	0.355	0.718	4.123	1.549	3.143

Table 10: Non-dimensional natural frequencies of SCSC, SCSS and SSSS FG-sandwich plates.

Core	BCs	a/h	h/l	Scheme								
				2-1-1			1-1-1			1-2-1		
				p=0	1	10	p=0	1	10	p=0	1	10
Ceramic	SCSC	5	1	33.722	28.755	24.199	33.722	29.363	25.426	33.722	30.930	28.506
			2	20.791	17.451	14.536	20.791	17.844	15.317	20.791	18.823	17.189
			∞	13.965	10.969	8.563	13.965	11.214	8.785	13.965	11.981	10.065
		20	1	38.741	33.710	28.561	38.741	34.504	30.292	38.741	36.250	33.932
			2	24.291	20.089	16.541	24.291	20.553	17.379	24.291	21.755	19.616
			∞	16.920	12.563	9.539	16.920	12.833	9.688	16.920	13.839	11.224
	SCSS	5	1	25.091	22.603	19.467	25.091	23.150	20.784	25.091	24.207	23.186
			2	17.441	14.593	12.117	17.441	14.924	12.765	17.441	15.755	14.343
			∞	12.014	9.282	7.178	12.014	9.486	7.342	12.014	10.164	8.442
		20	1	31.699	27.594	23.382	31.699	28.246	24.807	31.699	29.674	27.787
			2	19.898	16.448	13.538	19.898	16.828	14.223	19.898	17.813	16.056
			∞	13.887	10.292	7.807	13.887	10.512	7.927	13.887	11.339	9.186
	SSSS	5	1	23.571	20.227	17.044	23.571	20.674	17.980	23.571	21.759	20.151
			2	14.831	12.385	10.270	14.831	12.664	10.806	14.831	13.376	12.152
			∞	10.372	7.932	6.114	10.372	8.099	6.221	10.372	8.694	7.169
		20	1	26.493	23.072	19.558	26.493	23.614	20.743	26.493	24.807	23.235
			2	16.640	13.757	11.331	16.640	14.069	11.888	16.640	14.894	13.421
			∞	11.625	8.615	6.550	11.625	8.791	6.626	11.625	9.484	7.679
FG	SCSC	5	1	25.129	25.254	25.196	27.582	27.323	26.922	28.881	27.392	25.641
			2	14.916	15.038	15.154	16.531	16.256	16.033	17.439	16.358	15.380
			∞	9.094	9.306	9.448	10.219	10.005	9.900	10.994	10.176	9.578
		20	1	28.789	28.648	28.525	31.900	31.219	30.591	33.511	31.316	29.056
			2	17.032	17.242	17.552	18.907	18.558	18.431	20.045	18.720	17.776
			∞	10.498	11.077	11.793	11.688	11.574	11.870	12.668	11.835	11.816
	SCSS	5	1	19.274	18.969	18.614	21.388	20.853	20.237	22.374	20.857	19.033
			2	12.403	12.514	12.626	13.776	13.529	13.339	14.561	13.625	12.809
			∞	7.689	7.945	8.168	8.629	8.475	8.461	9.310	8.635	8.253
		20	1	23.547	23.427	23.323	26.101	25.535	25.015	27.423	25.615	23.757
			2	13.938	14.112	14.369	15.476	15.188	15.086	16.410	15.322	14.552
			∞	8.600	9.085	9.688	9.574	9.484	9.736	10.378	9.698	9.702
	SSSS	5	1	17.378	17.355	17.226	19.223	18.901	18.487	20.187	18.963	17.552
			2	10.559	10.666	10.771	11.707	11.514	11.373	12.370	11.595	10.925
			∞	6.675	6.939	7.181	7.428	7.351	7.402	7.997	7.484	7.245
		20	1	19.737	19.645	19.560	21.850	21.398	20.981	22.944	21.459	19.925
			2	11.748	11.910	12.129	12.994	12.793	12.737	13.754	12.896	12.285
			∞	7.337	7.761	8.269	8.093	8.076	8.326	8.735	8.239	8.286

Table 11: Non-dimensional natural frequencies of SCSF, SSSF and SFSF FG-sandwich plates.

Core	BCs	a/h	h/l	Scheme 2-1-1 p=0	2-1-1 1	2-1-1 10	1-1-1 p=0	1-1-1 1	1-1-1 10	1-2-1 p=0	1-2-1 1	1-2-1 10
Ceramic	SCSF	5	1	17.412	15.193	12.922	17.412	15.535	13.686	17.412	16.306	15.288
			2	10.381	8.786	7.352	10.381	8.991	7.784	10.381	9.474	8.725
			∞	6.928	5.239	4.008	6.928	5.353	4.085	6.928	5.756	4.716
		20	1	19.347	17.064	14.565	19.347	17.471	15.496	19.347	18.317	17.316
			2	11.456	9.648	8.037	11.456	9.874	8.486	11.456	10.421	9.544
			∞	7.496	5.543	4.202	7.496	5.662	4.265	7.496	6.110	4.943
	SSSF	5	1	16.046	14.015	11.929	16.046	14.330	12.631	16.046	15.040	14.111
			2	9.567	8.095	6.774	9.567	8.282	7.165	9.567	8.728	8.033
			∞	6.438	4.857	3.716	6.438	4.960	3.778	6.438	5.336	4.365
		20	1	17.705	15.611	13.324	17.705	15.983	14.170	17.705	16.758	15.837
			2	10.506	8.843	7.367	10.506	9.048	7.771	10.506	9.551	8.741
			∞	6.907	5.110	3.877	6.907	5.217	3.929	6.907	5.630	4.554
	SFSF	5	1	13.891	12.221	10.438	13.891	12.499	11.071	13.891	13.106	12.360
			2	8.027	6.825	5.729	8.027	6.985	6.073	8.027	7.355	6.802
			∞	5.367	4.037	3.081	5.367	4.124	3.137	5.367	4.439	3.626
		20	1	14.960	13.241	11.323	14.960	13.558	12.054	14.960	14.207	13.464
			2	8.727	7.380	6.165	8.727	7.553	6.516	8.727	7.966	7.322
			∞	5.699	4.213	3.192	5.699	4.303	3.241	5.699	4.644	3.756
FG	SCSF	5	1	13.097	13.011	12.855	14.482	14.219	13.859	15.161	14.242	13.113
			2	7.425	7.439	7.468	8.277	8.089	7.928	8.743	8.141	7.585
			∞	4.350	4.547	4.758	4.866	4.800	4.855	5.266	4.900	4.786
		20	1	14.571	14.420	14.266	16.160	15.782	15.391	16.942	15.811	14.555
			2	8.182	8.222	8.302	9.090	8.899	8.784	9.607	8.960	8.425
			∞	4.634	4.901	5.236	5.157	5.111	5.253	5.592	5.228	5.241
	SSSF	5	1	12.129	12.052	11.917	13.384	13.156	12.846	13.999	13.173	12.156
			2	6.874	6.893	6.924	7.645	7.484	7.349	8.066	7.530	7.032
			∞	4.070	4.262	4.467	4.532	4.487	4.554	4.896	4.578	4.492
		20	1	13.351	13.219	13.083	14.794	14.459	14.111	15.507	14.484	13.347
			2	7.531	7.575	7.652	8.349	8.189	8.095	8.817	8.242	7.765
			∞	4.312	4.563	4.871	4.777	4.751	4.893	5.169	4.854	4.879
	SFSF	5	1	10.556	10.458	10.312	11.659	11.441	11.148	12.189	11.451	10.527
			2	5.777	5.776	5.789	6.436	6.287	6.158	6.791	6.323	5.883
			∞	3.358	3.520	3.701	3.751	3.704	3.761	4.061	3.784	3.719
		20	1	11.308	11.177	11.041	12.542	12.244	11.928	13.142	12.262	11.269
			2	6.261	6.281	6.330	6.955	6.807	6.710	7.346	6.850	6.427
			∞	3.522	3.725	3.982	3.919	3.885	3.995	4.249	3.973	3.985

Table 12: Non-dimensional buckling loads of SCSC, SCSS and SSSS FG-sandwich plates.

Core	BCs	a/h	h/l	Scheme								
				2-1-1			1-1-1			1-2-1		
				p=0	1	10	p=0	1	10	p=0	1	10
Ceramic	SCSC	5	1	74.643	46.286	28.286	74.643	48.286	31.214	74.643	53.571	39.214
			2	28.536	17.250	10.357	28.536	18.036	11.500	28.536	20.036	14.464
			∞	13.143	6.957	3.671	13.143	7.275	3.862	13.143	8.302	5.068
		20	1	95.657	61.943	38.324	95.657	64.914	43.124	95.657	71.657	54.095
			2	37.638	22.000	12.857	37.638	23.029	14.191	37.638	25.810	18.076
			∞	18.297	8.620	4.280	18.297	8.995	4.415	18.297	10.462	5.926
	SCSS	5	1	53.500	33.429	20.500	53.500	34.929	22.643	53.500	38.714	28.500
			2	20.929	12.571	7.500	20.929	13.143	8.321	20.929	14.643	10.500
			∞	10.055	5.160	2.676	10.055	5.392	2.799	10.055	6.186	3.697
		20	1	66.705	43.238	26.743	66.705	45.295	30.095	66.705	49.981	37.791
			2	26.305	15.371	8.971	26.305	16.076	9.905	26.305	18.019	12.610
			∞	12.824	6.022	2.986	12.824	6.284	3.079	12.824	7.312	4.134
	SSSS	5	1	41.143	25.857	15.857	41.143	27.000	17.571	41.143	29.929	22.143
			2	16.321	9.750	5.786	16.321	10.214	6.429	16.321	11.393	8.107
			∞	8.011	4.035	2.081	8.011	4.209	2.154	8.011	4.844	2.857
		20	1	50.210	32.571	20.152	50.210	34.133	22.667	50.210	37.638	28.457
			2	19.810	11.581	6.762	19.810	12.114	7.448	19.810	13.581	9.486
			∞	9.676	4.545	2.265	9.676	4.733	2.316	9.676	5.509	3.112
FG	SCSC	5	1	42.421	36.679	31.836	50.457	42.543	36.179	55.057	42.693	32.929
			2	14.964	12.957	11.379	18.257	15.104	12.754	20.239	15.271	11.721
			∞	5.668	5.048	4.485	7.116	5.831	4.941	8.206	6.023	4.614
		20	1	52.914	44.800	38.286	64.914	53.181	44.038	71.619	53.486	39.695
			2	18.514	16.229	14.495	22.819	18.800	15.981	25.638	19.124	14.876
			∞	7.049	6.715	6.565	8.731	7.326	6.646	10.253	7.657	6.588
	SCSS	5	1	30.214	26.021	22.521	36.164	30.321	25.650	39.557	30.443	23.314
			2	10.811	9.375	8.257	13.236	10.925	9.225	14.721	11.064	8.504
			∞	4.208	3.816	3.474	5.263	4.341	3.746	6.100	4.499	3.552
		20	1	36.876	31.200	26.667	45.257	37.067	30.667	49.943	37.295	27.657
			2	12.914	11.314	10.114	15.905	13.105	11.143	17.886	13.333	10.381
			∞	4.925	4.700	4.608	6.098	5.120	4.653	7.165	5.353	4.621
	SSSS	5	1	23.307	20.043	17.329	27.929	23.386	19.757	30.557	23.479	17.936
			2	8.471	7.375	6.511	10.321	8.561	7.261	11.468	8.664	6.700
			∞	3.401	3.121	2.875	4.181	3.503	3.073	4.822	3.624	2.932
		20	1	27.924	23.657	20.191	34.171	28.038	23.238	37.676	28.191	20.952
			2	9.886	8.686	7.771	12.095	10.019	8.571	13.543	10.171	7.962
			∞	3.857	3.691	3.613	4.693	3.995	3.661	5.464	4.160	3.626

Table 13: Non-dimensional buckling loads of SCSF, SSSF and SFSF FG-sandwich plates.

Core	BCs	a/h	h/l	Scheme 2-1-1 p=0	2-1-1 1	2-1-1 10	1-1-1 p=0	1-1-1 1	1-1-1 10	1-2-1 p=0	1-2-1 1	1-2-1 10
Ceramic	SCSF	5	1	34.571	22.429	14.000	34.571	23.500	15.643	34.571	25.857	19.571
			2	11.964	7.393	4.500	11.964	7.750	5.071	11.964	8.607	6.357
			∞	4.971	2.427	1.227	4.971	2.535	1.272	4.971	2.931	1.697
		20	1	30.286	29.714	18.857	43.810	31.238	21.524	43.810	34.286	26.857
			2	14.095	8.762	5.333	14.095	9.143	5.905	14.095	10.191	7.524
			∞	5.566	2.603	1.288	5.566	2.716	1.327	5.566	3.162	1.784
	SSSF	5	1	31.214	20.286	12.643	31.214	21.143	14.071	31.214	23.357	17.643
			2	10.821	6.714	4.071	10.821	7.036	4.607	10.821	7.786	5.750
			∞	4.627	2.254	1.139	4.627	2.351	1.178	4.627	2.721	1.572
		20	1	30.286	26.667	16.762	39.238	27.810	19.048	39.238	30.667	23.810
			2	12.762	7.905	4.762	12.762	8.286	5.333	12.762	9.143	6.762
			∞	5.139	2.404	1.192	5.139	2.507	1.225	5.139	2.919	1.646
	SFSF	5	1	29.714	19.500	12.214	29.714	20.357	13.643	29.714	22.429	17.071
			2	9.643	5.964	3.714	9.643	6.321	4.179	9.643	7.000	5.250
			∞	4.139	2.005	1.009	4.139	2.094	1.046	4.139	2.424	1.397
		20	1	30.286	24.952	16.000	36.571	26.286	18.095	36.571	28.762	22.667
			2	11.333	7.143	4.286	11.333	7.429	4.857	11.333	8.286	6.095
			∞	4.544	2.124	1.050	4.544	2.216	1.082	4.544	2.580	1.455
FG	SCSF	5	1	20.150	17.007	14.386	24.286	20.164	16.721	26.450	20.186	14.971
			2	6.282	5.357	4.646	7.768	6.339	5.261	8.621	6.404	4.800
			∞	1.983	1.850	1.754	2.466	2.054	1.825	2.880	2.140	1.775
		20	1	25.524	21.143	17.714	31.429	25.524	20.762	34.286	25.524	18.476
			2	7.333	6.286	5.429	9.048	7.429	6.191	10.095	7.524	5.619
			∞	2.129	2.037	2.004	2.635	2.214	2.017	3.098	2.316	2.008
	SSSF	5	1	18.264	15.471	13.121	21.936	18.279	15.221	23.879	18.293	13.650
			2	5.732	4.893	4.246	7.061	5.779	4.811	7.825	5.836	4.386
			∞	1.861	1.740	1.652	2.302	1.927	1.718	2.683	2.005	1.672
		20	1	22.857	19.048	16.000	28.000	22.857	18.667	30.667	22.857	16.571
			2	6.667	5.714	4.952	8.286	6.762	5.619	9.143	6.857	5.143
			∞	1.989	1.904	1.872	2.449	2.066	1.887	2.871	2.158	1.877
	SFSF	5	1	17.629	14.921	12.614	21.121	17.621	14.686	22.950	17.614	13.136
			2	5.139	4.361	3.761	6.343	5.175	4.282	7.021	5.221	3.889
			∞	1.639	1.536	1.466	2.036	1.699	1.516	2.381	1.771	1.481
		20	1	21.524	17.714	14.857	26.286	21.524	17.524	28.762	21.524	15.429
			2	6.000	5.143	4.381	7.429	6.000	5.048	8.191	6.095	4.571
			∞	1.737	1.662	1.636	2.150	1.806	1.646	2.528	1.890	1.639

List of figures

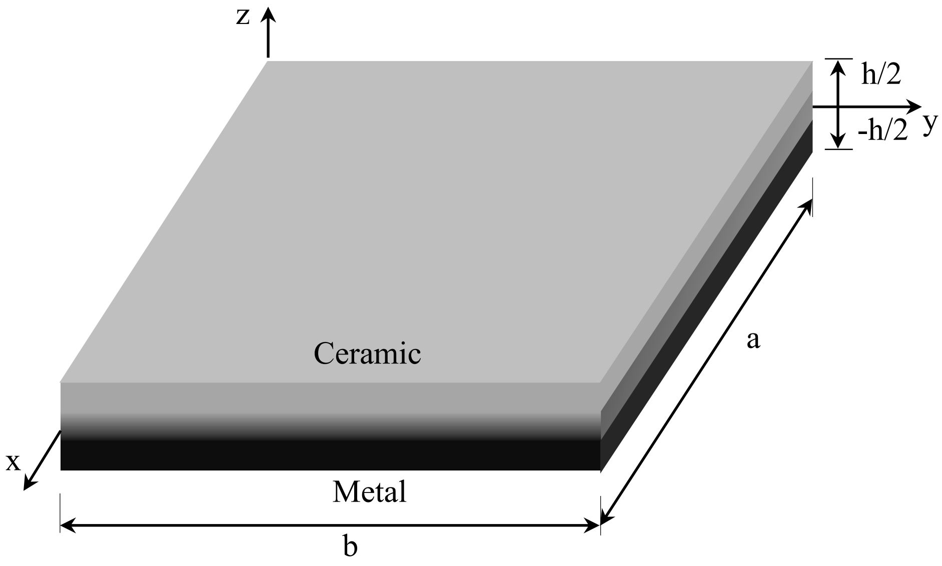

Fig. 1: Geometry and co-ordinates of FG-core (1-1-1) plates.

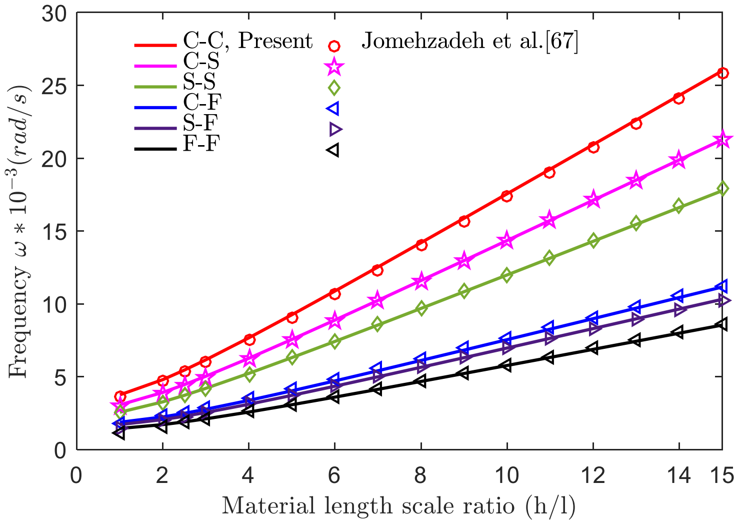

Fig. 2: The size effect on the fundamental frequencies of epoxy plates under various BCs.

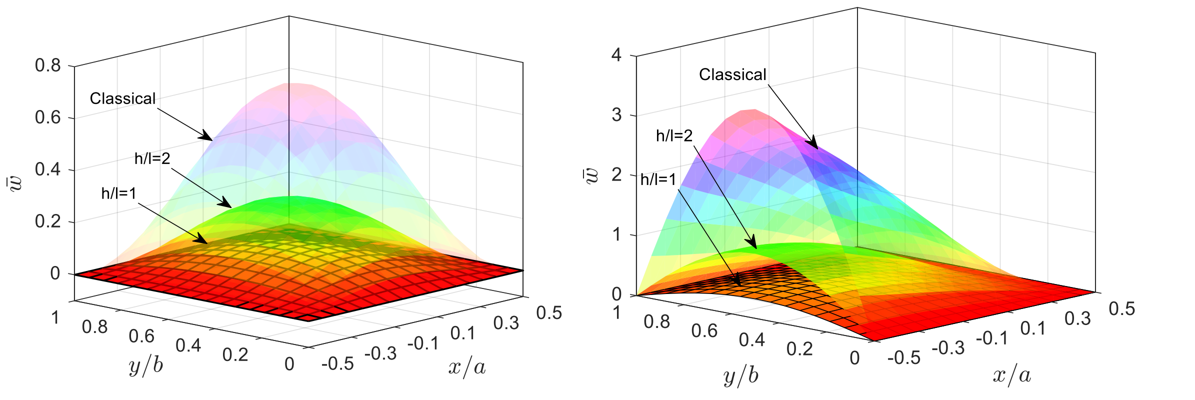

a. SCSC b. SCSF

Fig. 3: Size effect on the deflections of FG-core (1-1-1) plates.

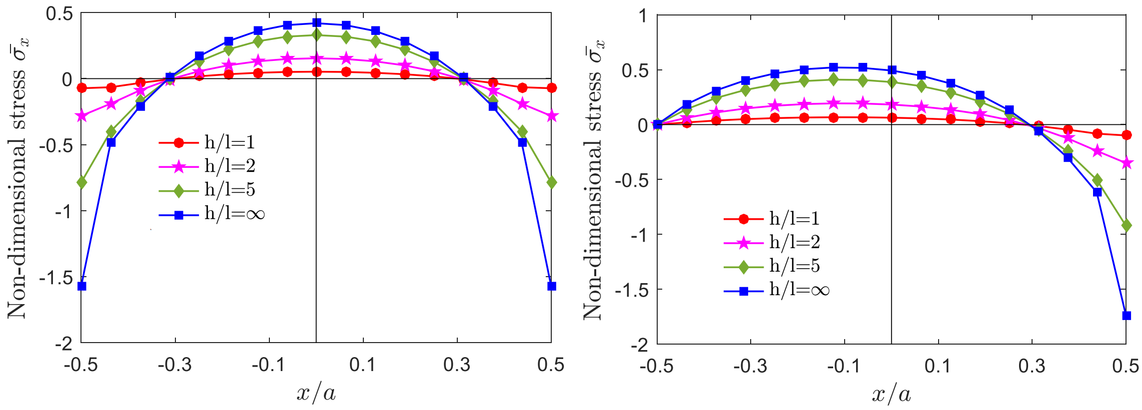

i. SCSC *ii. SCSS*

a. $\bar{\sigma}_x\left(x, b/2, h/2\right)$

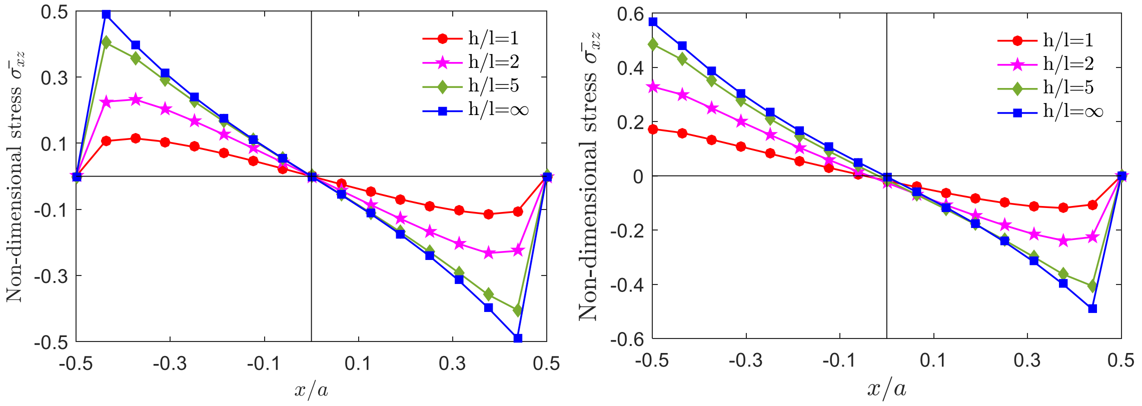

i. SCSC *ii. SCSS*

b. $\bar{\sigma}_{xz}\left(x, b/2, 0\right)$

Fig. 4: Size effect on the stresses of ceramic-core (1-1-1) plates (a/h=5).

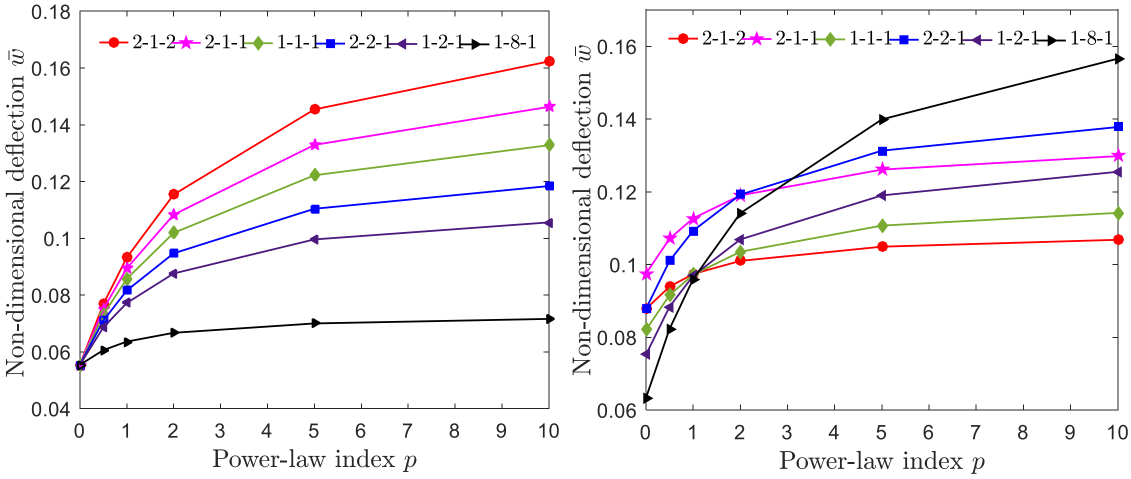

a. Ceramic-core *b. FG-core*

Fig. 5: Non-dimensional deflections of various FG-sandwich plates (a/h=5, h/l=1, SCSC).

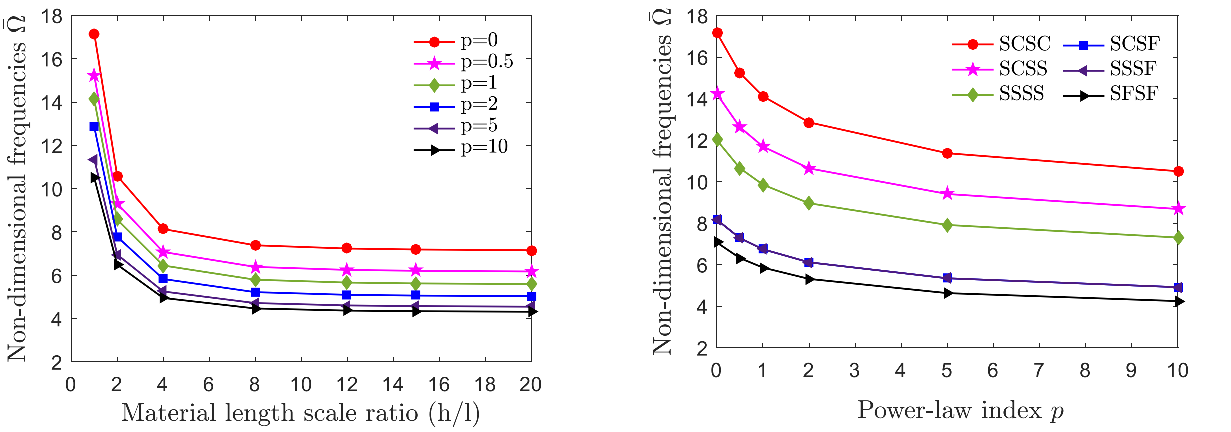

a. SCSC *b.* $h/l=1$

Fig. 6: Effects of power-law index and boundary conditions on the vibration of Al/Al_2O_3 plates (a/h=5).

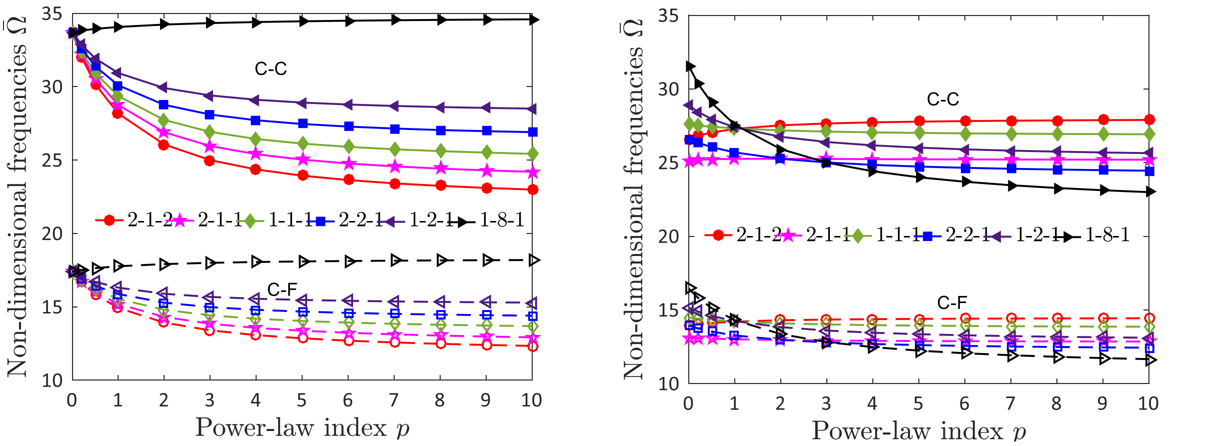

a. Ceramic-core plates *b. FG-core plates*

Fig. 7: Non-dimensional natural frequencies of Al/Al_2O_3 sandwich microplates (a/h=5, h/l=1).

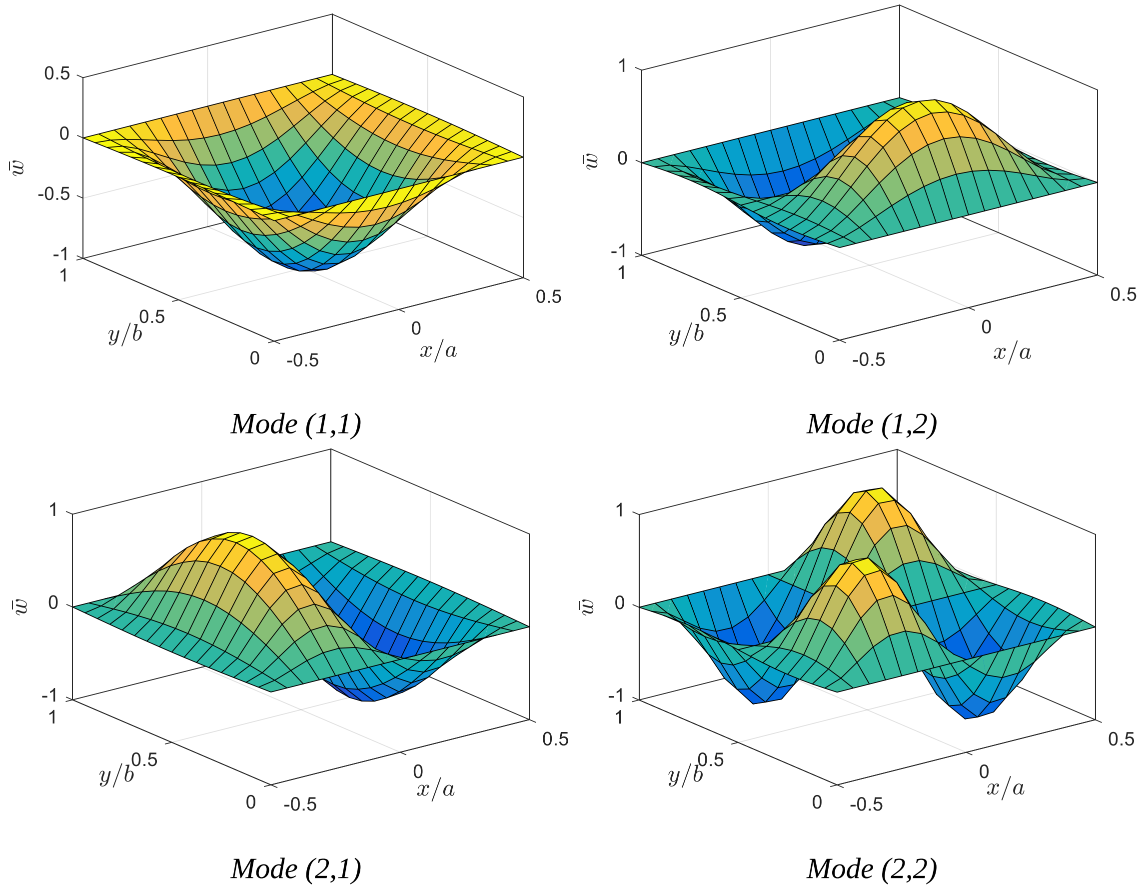

Fig. 8: The first four mode shapes of SCSC FG microplates (a/h=10, h/l=2).

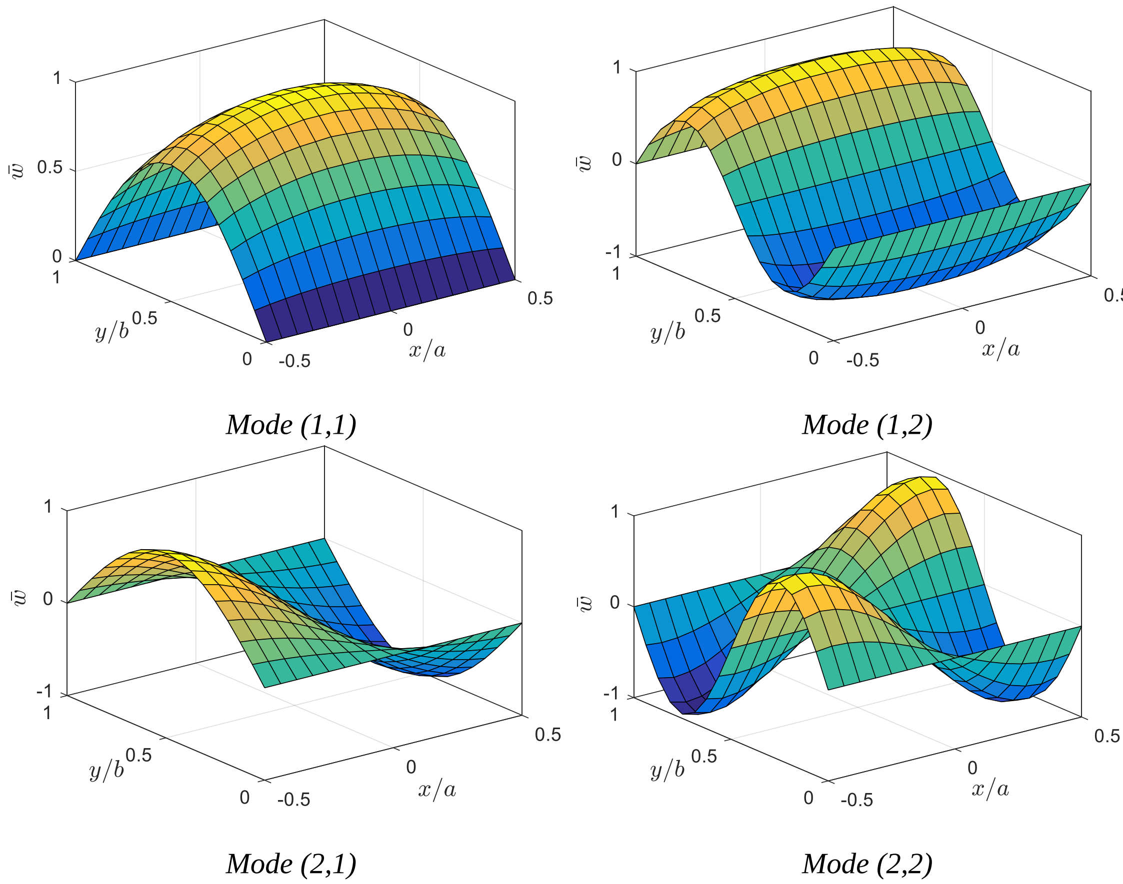

Fig. 9: The first four mode shapes of SFSF FG microplates (a/h=10, h/l=2).

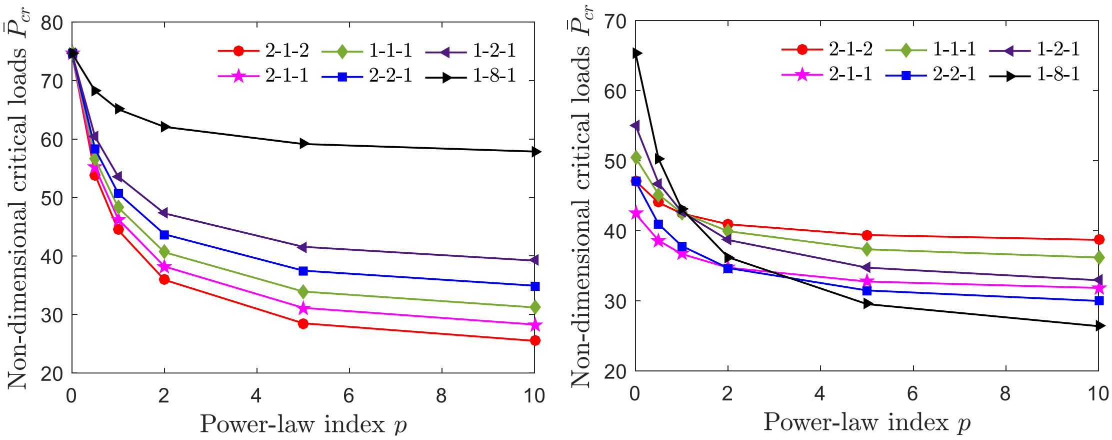

a. Ceramic core *b. FG-core*

Fig. 10: Non-dimensional buckling loads of Al/Al_2O_3 sandwich microplates (a/h=5, h/l=1).

Appendix A

$$N_{xx}=A_{11}\frac{\partial U}{\partial x}+A_{12}\frac{\partial V}{\partial y}-B_{11}\frac{\partial^2 W_b}{\partial x^2}-B_{12}\frac{\partial^2 W_b}{\partial y^2}-B_{11}^s\frac{\partial^2 W_s}{\partial x^2}-B_{12}^s\frac{\partial^2 W_s}{\partial y^2} \tag{A1}$$

$$N_{yy}=A_{12}\frac{\partial U}{\partial x}+A_{22}\frac{\partial V}{\partial y}-B_{12}\frac{\partial^2 W_b}{\partial x^2}-B_{22}\frac{\partial^2 W_b}{\partial y^2}-B_{12}^s\frac{\partial^2 W_s}{\partial x^2}-B_{22}^s\frac{\partial^2 W_s}{\partial y^2} \tag{A2}$$

$$N_{xy}=A_{66}\left(\frac{\partial U}{\partial y}+\frac{\partial V}{\partial x}\right)-2B_{66}\frac{\partial^2 W_b}{\partial x\partial y}-2B_{66}^s\frac{\partial^2 W_s}{\partial x\partial y} \tag{A3}$$

$$M_{xx}=B_{11}\frac{\partial U}{\partial x}+B_{12}\frac{\partial V}{\partial y}-D_{11}\frac{\partial^2 W_b}{\partial x^2}-D_{12}\frac{\partial^2 W_b}{\partial y^2}-D_{11}^s\frac{\partial^2 W_s}{\partial x^2}-D_{12}^s\frac{\partial^2 W_s}{\partial y^2} \tag{A4}$$

$$M_{yy}=B_{12}\frac{\partial U}{\partial x}+B_{22}\frac{\partial V}{\partial y}-D_{12}\frac{\partial^2 W_b}{\partial x^2}-D_{22}\frac{\partial^2 W_b}{\partial y^2}-D_{12}^s\frac{\partial^2 W_s}{\partial x^2}-D_{22}^s\frac{\partial^2 W_s}{\partial y^2} \tag{A5}$$

$$M_{xy}=B_{66}\left(\frac{\partial U}{\partial y}+\frac{\partial V}{\partial x}\right)-2D_{66}\frac{\partial^2 W_b}{\partial x\partial y}-2D_{66}^s\frac{\partial^2 W_s}{\partial x\partial y} \tag{A6}$$

$$P_{xx}=B_{11}^s\frac{\partial U}{\partial x}+B_{12}^s\frac{\partial V}{\partial y}-D_{11}^s\frac{\partial^2 W_b}{\partial x^2}-D_{12}^s\frac{\partial^2 W_b}{\partial y^2}-H_{11}\frac{\partial^2 W_s}{\partial x^2}-H_{12}\frac{\partial^2 W_s}{\partial y^2} \tag{A7}$$

$$P_{yy}=B_{12}^s\frac{\partial U}{\partial x}+B_{22}^s\frac{\partial V}{\partial y}-D_{12}^s\frac{\partial^2 W_b}{\partial x^2}-D_{22}^s\frac{\partial^2 W_b}{\partial y^2}-H_{12}\frac{\partial^2 W_s}{\partial x^2}-H_{22}\frac{\partial^2 W_s}{\partial y^2} \tag{A8}$$

$$P_{xy}=B_{66}^s\left(\frac{\partial U}{\partial y}+\frac{\partial V}{\partial x}\right)-2D_{66}^s\frac{\partial^2 W_b}{\partial x\partial y}-2H_{66}\frac{\partial^2 W_s}{\partial x\partial y} \tag{A9}$$

$$Q_{xz}=A_{55}^s\frac{\partial W_s}{\partial x} \tag{A10}$$

$$Q_{yz}=A_{44}^s\frac{\partial W_s}{\partial y} \tag{A11}$$

$$R_{xx}=2A_m\frac{\partial^2 W_b}{\partial x\partial y}+\left(A_m+B_m\right)\frac{\partial^2 W_s}{\partial x\partial y} \tag{A12}$$

$$R_{yy}=-2A_m\frac{\partial^2 W_b}{\partial x\partial y}-\left(A_m+B_m\right)\frac{\partial^2 W_s}{\partial x\partial y} \tag{A13}$$

$$R_{xy}=A_m\frac{\partial^2 W_b}{\partial y^2}+\frac{1}{2}\left(A_m+B_m\right)\frac{\partial^2 W_s}{\partial y^2}-A_m\frac{\partial^2 W_b}{\partial x^2}-\frac{1}{2}\left(A_m+B_m\right)\frac{\partial^2 W_s}{\partial x^2} \tag{A14}$$

$$R_{xz}=\frac{1}{2}A_m\frac{\partial^2 V}{\partial x^2}-\frac{1}{2}A_m\frac{\partial^2 U}{\partial x\partial y}-G_m\frac{\partial W_s}{\partial y} \tag{A15}$$

$$R_{yz}=\frac{1}{2}A_m\frac{\partial^2 V}{\partial x\partial y}-\frac{1}{2}A_m\frac{\partial^2 U}{\partial y^2}+G_m\frac{\partial W_s}{\partial x} \tag{A16}$$

$$S_{xx}=2B_m\frac{\partial^2 W_b}{\partial x\partial y}+\left(B_m+C_m\right)\frac{\partial^2 W_s}{\partial x\partial y} \tag{A17}$$

$$S_{yy}=-2B_m\frac{\partial^2 W_b}{\partial x\partial y}-\left(B_m+C_m\right)\frac{\partial^2 W_s}{\partial x\partial y} \tag{A18}$$

$$S_{xy}=B_m\frac{\partial^2 W_b}{\partial y^2}+\frac{1}{2}\left(B_m+C_m\right)\frac{\partial^2 W_s}{\partial y^2}-B_m\frac{\partial^2 W_b}{\partial x^2}-\frac{1}{2}\left(B_m+C_m\right)\frac{\partial^2 W_s}{\partial x^2} \tag{A19}$$

$$X_{xz}=-\frac{1}{2}G_m\frac{\partial^2 V}{\partial x^2}+\frac{1}{2}G_m\frac{\partial^2 U}{\partial x\partial y}+H_m\frac{\partial W_s}{\partial y} \tag{A20}$$

$$X_{yz}=-\frac{1}{2}G_m\frac{\partial^2 V}{\partial x\partial y}+\frac{1}{2}G_m\frac{\partial^2 U}{\partial y^2}-H_m\frac{\partial W_s}{\partial x} \tag{A21}$$

where

$$\left(A_{ij},A_{ij}^s,B_{ij},B_{ij}^s,D_{ij},D_{ij}^s,H_{ij}\right)=\int_{-h/2}^{h/2}\left(1,g^2,z,f,z^2,fz,f^2\right)Q_{ij}dz \tag{A22}$$

$$\left(K_{ij},L_{ij},L_{ij}^s,Z_{ij}\right)=\int_{-h/2}^{h/2}\left(1,z,f,\frac{\partial g}{\partial z}\right)\frac{\partial g}{\partial z}Q_{ij}dz \tag{A23}$$

$$\begin{aligned}&\left(A_m,B_m,C_m,D_m,E_m,F_m,G_m,H_m\right)\\&=\int_{-h/2}^{h/2}l^2\mu\left[1,\frac{\partial f}{\partial z},\left(\frac{\partial f}{\partial z}\right)^2,\frac{\partial f}{\partial z}g,g,g^2,\frac{\partial g}{\partial z},\left(\frac{\partial g}{\partial z}\right)^2\right]dz\end{aligned} \tag{A24}$$

Appendix B

$$a_1 = \frac{\beta^2 A_{66} + \frac{1}{4}\beta^4 A_m - I_0\omega^2}{A_{11} + \frac{1}{4}\beta^2 A_m}; a_2 = \frac{\beta\left(A_{12} + A_{66}\right) - \frac{1}{4}\beta^3 A_m}{A_{11} + \frac{1}{4}\beta^2 A_m}; a_3 = \frac{\frac{1}{4}\beta A_m}{A_{11} + \frac{1}{4}\beta^2 A_m};$$

$$a_4 = \frac{-\beta^2\left(B_{12} + 2B_{66}\right) + I_1\omega^2}{A_{11} + \frac{1}{4}\beta^2 A_m}; a_5 = \frac{B_{11}}{A_{11} + \frac{1}{4}\beta^2 A_m}; a_6 = \frac{-\beta^2\left(B_{12}^s + 2B_{66}^s\right) + J_1\omega^2}{A_{11} + \frac{1}{4}\beta^2 A_m};$$

$$a_7 = \frac{B_{11}^s}{A_{11} + \frac{1}{4}\beta^2 A_m}. \tag{B1}$$

$$\begin{aligned}
r_1 &= \left[c_3\left(e_4h_2 - e_2h_4\right) - e_3\left(c_4h_2 - c_2h_4\right) + h_3\left(c_4e_2 - c_2e_4\right)\right]/C_0 \\
r_2 &= \left[c_3\left(e_5h_2 - e_2h_5\right) - e_3\left(c_5h_2 - c_2h_5\right) + h_3\left(c_5e_2 - c_2e_5\right)\right]/C_0 \\
r_3 &= \left[c_3\left(e_6h_2 - e_2h_6\right) - e_3\left(c_6h_2 - c_2h_6\right) + h_3\left(c_6e_2 - c_2e_6\right)\right]/C_0 \\
r_4 &= \left[c_3\left(e_7h_2 - e_2h_7\right) - e_3\left(c_7h_2 - c_2h_7\right) + h_3\left(c_7e_2 - c_2e_7\right)\right]/C_0 \\
r_5 &= \left[c_3\left(e_8h_2 - e_2h_8\right) - e_3\left(c_8h_2 - c_2h_8\right) + h_3\left(c_8e_2 - c_2e_8\right)\right]/C_0 \\
r_6 &= \left[c_3\left(e_9h_2 - e_2h_9\right) - e_3\left(c_9h_2 - c_2h_9\right) + h_3\left(c_9e_2 - c_2e_9\right)\right]/C_0 \\
r_7 &= \left[c_3\left(e_{10}h_2 - e_2h_{10}\right) - e_3\left(c_{10}h_2 - c_2h_{10}\right) + h_3\left(c_{10}e_2 - c_2e_{10}\right)\right]/C_0 \\
r_8 &= \left[c_3\left(e_{11}h_2 - e_2h_{11}\right) + e_3c_2h_{11} - h_3c_2e_{11}\right]/C_0
\end{aligned} \tag{B2}$$

$$\begin{aligned}
s_1 &= \left[c_1\left(e_4h_3 - e_3h_4\right) - e_1\left(c_4h_3 - c_3h_4\right) + h_1\left(c_4e_3 - c_3e_4\right)\right]/C_0 \\
s_2 &= \left[c_1\left(e_5h_3 - e_3h_5\right) - e_1\left(c_5h_3 - c_3h_5\right) + h_1\left(c_5e_3 - c_3e_5\right)\right]/C_0 \\
s_3 &= \left[c_1\left(e_6h_3 - e_3h_6\right) - e_1\left(c_6h_3 - c_3h_6\right) + h_1\left(c_6e_3 - c_3e_6\right)\right]/C_0 \\
s_4 &= \left[c_1\left(e_7h_3 - e_3h_7\right) - e_1\left(c_7h_3 - c_3h_7\right) + h_1\left(c_7e_3 - c_3e_7\right)\right]/C_0 \\
s_5 &= \left[c_1\left(e_8h_3 - e_3h_8\right) - e_1\left(c_8h_3 - c_3h_8\right) + h_1\left(c_8e_3 - c_3e_8\right)\right]/C_0 \\
s_6 &= \left[c_1\left(e_9h_3 - e_3h_9\right) - e_1\left(c_9h_3 - c_3h_9\right) + h_1\left(c_9e_3 - c_3e_9\right)\right]/C_0 \\
s_7 &= \left[c_1\left(e_{10}h_3 - e_3h_{10}\right) - e_1\left(c_{10}h_3 - c_3h_{10}\right) + h_1\left(c_{10}e_3 - c_3e_{10}\right)\right]/C_0 \\
s_8 &= \left[c_1\left(e_{11}h_3 - e_3h_{11}\right) + e_1c_3h_{11} - h_1c_3e_{11}\right]/C_0
\end{aligned} \tag{B3}$$

$$t_1=\left[c_1\left(e_2h_4-h_2e_4\right)-e_1\left(c_2h_4-h_2c_4\right)+h_1\left(c_2e_4-e_2c_4\right)\right]/C_0$$
$$t_2=\left[c_1\left(e_2h_5-h_2e_5\right)-e_1\left(c_2h_5-h_2c_5\right)+h_1\left(c_2e_5-e_2c_5\right)\right]/C_0$$
$$t_3=\left[c_1\left(e_2h_6-h_2e_6\right)-e_1\left(c_2h_6-h_2c_6\right)+h_1\left(c_2e_6-e_2c_6\right)\right]/C_0$$
$$t_4=\left[c_1\left(e_2h_7-h_2e_7\right)-e_1\left(c_2h_7-h_2c_7\right)+h_1\left(c_2e_7-e_2c_7\right)\right]/C_0$$
$$t_5=\left[c_1\left(e_2h_8-h_2e_8\right)-e_1\left(c_2h_8-h_2c_8\right)+h_1\left(c_2e_8-e_2c_8\right)\right]/C_0$$
$$t_6=\left[c_1\left(e_2h_9-h_2e_9\right)-e_1\left(c_2h_9-h_2c_9\right)+h_1\left(c_2e_9-e_2c_9\right)\right]/C_0$$
$$t_7=\left[c_1\left(e_2h_{10}-h_2e_{10}\right)-e_1\left(c_2h_{10}-h_2c_{10}\right)+h_1\left(c_2e_{10}-e_2c_{10}\right)\right]/C_0$$
$$t_8=\left[c_1\left(e_2h_{11}-h_2e_{11}\right)-e_1c_2h_{11}+h_1c_2e_{11}\right]/C_0 \tag{B4}$$

$$b_1=\frac{\beta\left(A_{12}+A_{66}\right)-\frac{1}{4}\beta^3A_m}{\frac{1}{4}A_m};b_2=\beta;b_3=\frac{-\beta^2A_{22}+I_0\omega^2}{\frac{1}{4}A_m};b_4=\frac{A_{66}+\frac{1}{4}\beta^2A_m}{\frac{1}{4}A_m};$$

$$b_5=\frac{\beta^3B_{22}-\beta I_1\omega^2}{\frac{1}{4}A_m};b_6=\frac{-\beta\left(B_{12}+2B_{66}\right)}{\frac{1}{4}A_m};b_7=\frac{\beta^3B_{22}^s-\beta J_1\omega^2}{\frac{1}{4}A_m};b_8=\frac{-\beta\left(B_{12}^s+2B_{66}^s\right)}{\frac{1}{4}A_m}. \tag{B5}$$

$$c_1=1-a_3b_2;c_2=-a_5b_2;c_3=-a_7b_2;c_4=b_1+a_1b_2;c_5=b_3;$$

$$c_6=a_2b_2+b_4;c_7=b_5;c_8=a_4b_2+b_6;c_9=b_7;c_{10}=a_6b_2+b_8. \tag{B6}$$

$$d_1=\left(D_{11}+A_m\right);d_2=\left[D_{11}^s+\frac{1}{2}\left(A_m+B_m\right)\right];d_3=\left[-\beta^2\left(B_{12}+2B_{66}\right)+I_1\omega^2\right];d_4=B_{11};$$
$$d_5=\left(\beta^3B_{22}-\beta I_1\omega^2\right);d_6=-\beta\left(B_{12}+2B_{66}\right);d_7=\left[-\beta^4\left(D_{22}+A_m\right)+I_0\omega^2+\beta^2I_2\omega^2-\gamma_2P_0\beta^2\right];$$
$$d_8=\left[\beta^2\left(2D_{12}+4D_{66}+2A_m\right)-I_2\omega^2+\gamma_1P_0\right];$$
$$d_9=\left\{-\beta^4\left[D_{22}^s+\frac{1}{2}\left(A_m+B_m\right)\right]+I_0\omega^2+\beta^2J_2\omega^2-\gamma_2P_0\beta^2\right\};$$

$$d_{10}=\left[\beta^2\left(2D_{12}^s+4D_{66}^s\right)-J_2\omega^2+\gamma_1P_0\right];d_{11}=Q_m \tag{B7}$$

$$g_1 = D_{11}^s + \frac{1}{2}\left(A_m + B_m\right); g_2 = H_{11} + \frac{1}{4}\left(A_m + 2B_m + C_m\right); g_3 = -\beta^2\left(B_{12}^s + 2B_{66}^s\right) + J_1\omega^2; g_4 = B_{11}^s;$$

$$g_5 = \beta^3 B_{22}^s - \beta J_1\omega^2; g_6 = -\beta\left(B_{12}^s + 2B_{66}^s\right); g_7 = -\beta^4\left[D_{22}^s + \frac{1}{2}\left(A_m + B_m\right)\right] + I_0\omega^2 + \beta^2 J_2\omega^2 - \gamma_2 P_0\beta^2;$$

$$g_8 = \beta^2\left(2D_{12}^s + 4D_{66}^s\right) - J_2\omega^2 + \gamma_1 P_0;$$

$$g_9 = -\beta^4\left[H_{22} + \frac{1}{4}\left(A_m + 2B_m + C_m\right)\right] - \beta^2\left(A_{44}^s + \frac{1}{4}H_m\right) + I_0\omega^2 + \beta^2 K_2\omega^2 - \gamma_2 P_0\beta^2;$$

$$g_{10} = \left(A_{55}^s + \frac{1}{4}H_m\right) + \beta^2\left(2H_{12} + 4H_{66}\right) - K_2\omega^2 + \gamma_1 P_0; g_{11} = Q_m \tag{B8}$$

$$h_1 = a_3 g_4; h_2 = \left(g_1 - a_5 g_4\right); h_3 = \left(g_2 - a_7 g_4\right); h_4 = \left(a_1 g_4 + g_3\right); h_5 = g_5;$$

$$h_6 = \left(a_2 g_4 + g_6\right); h_7 = g_7; h_8 = \left(a_4 g_4 + g_8\right); h_9 = g_9; h_{10} = \left(a_6 g_4 + g_{10}\right); h_{11} = g_{11}. \tag{B9}$$